QUASI-STEADY-STATE MODELING AND CONTROL OF

A FUEL CELL/BATTERY HYBRID SYSTEM FOR

RESIDENTIAL APPLICATION

By

ZHI YANG

A thesis submitted in partial fulfillment of

the requirements for the degree of

MASTER OF SCIENCE IN ELECTRICAL ENGINEERING

WASHINGTON STATE UNIVERSITY

School of Electrical Engineering and Computer Science

DECEMBER 2009

To the Faculty of Washington State University:

The members of the Committee appointed to examine the thesis of ZHI YANG find it satisfactory and recommend that it be accepted.

———————————————————
Patrick D. Pedrow ,Chair

———————————————————
Su Ha

———————————————————
Mani Venkatasubramanian

———————————————————
Mark Grimes

ACKNOWLEDGMENT

QUASI-STEADY-STATE MODELING AND CONTROL OF

A FUEL CELL/BATTERY HYBRID SYSTEM FOR

RESIDENTIAL APPLICATION

ABSTRACT

By ZHI YANG, M.S.
Washington State University
December 2009

Chair: Patrick D. Pedrow

The aim of this thesis is modeling and control of a fuel cell/battery hybrid system for residential application. In this thesis, MATLAB$^®$ and Simulink$^®$ have been used to produce a comprehensive dynamic system model giving in-depth information on a 5 kW fuel cell/battery hybrid power supply operating isolated from the main electric power grid. Sub-system blocks include fuel cell, fuel reformer, DC/DC booster, lead acid battery and a sinusoidal pulse width modulation DC/AC inverter with associated control and integration. A supervisory power controller based on a fuzzy logic algorithm was designed to determine the fuel cell output power in terms of the average active load power requirement and estimated battery state of charge (SOC) using the extended kalman filter (EKF) method. Simulation results with typical waveforms show that the integrated model with control is able to operate the fuel cell near maximum power points and keep the SOC of the battery within a prescribed range. Complicating factors in the simulation include the extended computation time due to power electronic devices.

TABLE OF CONTENTS

LIST OF TABLES

LIST OF FIGURES

CHAPTER 1 INTRODUCTION

Portable and auxiliary power supplies not connected to the electric power grid are needed for applications that include battery recharging, military missions, and recreation vehicles. In addition to the nation's quest for energy independence, there continues to be a significant push to preserve and protect our environment using alternative energy sources. Hydrogen fuel cells are ideal for these applications since they are quiet directly converting the chemical energy stored in hydrogen to electrical energy. However, limited by their inherent characteristics, fuel cells have a poor response to instantaneous power demands due to chemical processes. The combination of fuel cells with batteries yields a hybrid power source that makes the best use of the advantages of each individual device and may meet the requirements regarding both high power and high energy densities [1].

Various schemes of fuel cell/battery hybrid power systems have been recently investigated for such purposes. In Ref. [2] a topology placing the fuel cell at the maximum power point with minimum fuel flow for fuel cell/battery hybrid system is proposed. In Ref. [3], a load transient mitigation technique for stand-alone fuel cell (FC)–battery power generation systems is described. In Ref. [4], a PEM fuel cell power system is integrated with a PWM DC/DC converter. In Ref. [5], a fuzzy logic algorithm has been used to manage the power split between the fuel cell and battery.

Complicating factors in the simulation include the extended computation time due to power electronic devices. Detailed behavior of a DC/AC inverter switching at 10 kHz or higher requires nanosecond time resolution. Time constants of the other chemical devices, such as the fuel processor, are in the range of tens of seconds, so a simulation over several minutes is necessary to get valuable results.

1

Several simplifications were proposed to reduce the computational burden. In Ref. [4], a PEM fuel cell power system is integrated with a PWM DC/DC converter but without a DC/AC inverter. In Ref. [6], switching power converters are implemented into the hybrid system but a transient fuel cell stack model is not provided. These simplifications fast the simulation but some valuable information may be lost. For example, the simplified inverter model will not give any information about the harmonic content on the input side. However, this information is important because the harmonic currents caused by the switches will cause large charging and discharging current into and out of the battery, thus affect the estimation of battery SOC.

An integrated model which includes not only the detail power electronic devices but also a transient fuel cell model is needed to fully study the hybrid system. The major feature of this thesis work is that we present a relatively comprehensive dynamic model including power electronic devices with associated control strategies. The primary target is to operate the fuel cell near the maximum power point and to keep the SOC of the battery within an accepted range.

This thesis is organized as follows. Chapter 2 explains the complete dynamic model and control of each component of the hybrid system. The simulation results for DC load and AC load are presented in Chapter 3 individually. The final discussion and conclusions are given in Chapter 4.

CHAPTER 2 MODELING AND CONTROL OF THE HYBRID SYSTEM

2.1 INTRODUCTION

Modeling and control of the fuel cell/battery hybrid system is shown in Figure 2-1. After considering the estimated SOC and average active load power, the fuzzy logic controller determines how much power the fuel cell stack should provide. According to a fuel cell characteristic look up table, the reformer tunes the hydrogen flow rate and the booster adjusts the input current at specific values. The power generated by the fuel cell is boosted to a higher voltage by a DC/DC converter and then the voltage is partially regulated by the battery, and finally it is conditioned to an ac voltage by the inverter.
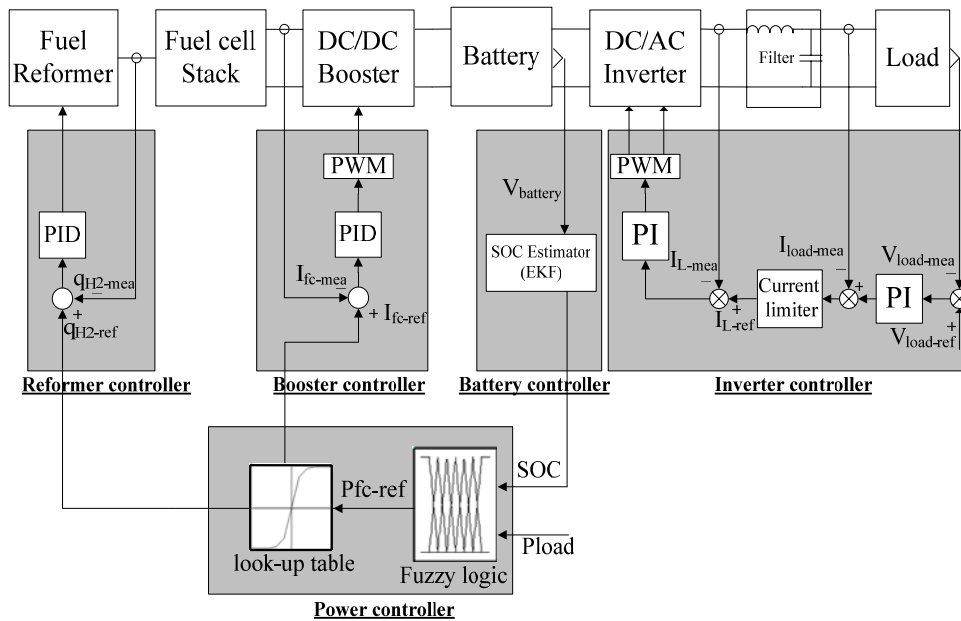
Figure 2-1: Modeling and control of the fuel cell/battery hybrid system.

2.2   PEM FUEL CELL

In Ref. [7], Padulles introduced a model for the SOFC. The model has been modified to simulate a PEM fuel cell. The parameters used in the mathematical modeling of the PEM fuel cell are as follows [7, 8, 9]:

q_{H_2}	molar flow of hydrogen [Kmol s^{-1}]
P_{H_2}	hydrogen partial pressure[atm]
K_{H_2}	hydrogen valve molar constant[Kmol (atms)$^{-1}$]
K_{an}	anode valve constant[$\sqrt{Kmol\ Kg}$ (atm s)$^{-1}$]
$q_{H_2}^{in}$	input hydrogen flow rate [Kmol s^{-1}]
$q_{H_2}^{out}$	output hydrogen flow rate [Kmol s^{-1}]
$q_{H_2}^{rea}$	hydrogen flow that reacts [Kmol s^{-1}].
I_{FC}	fuel cell current[A]
N_0	number of series fuel cells
Co_2	concentration of dissolved oxygen at the gas/liquid interface[mol cm^{-3}]
R_M	equivalent resistance of protons passing the solid membrane[Ω]
R_C	the equivalent resistance of electrons passing the collecting plates and carton electrodes[Ω]
F	Faraday constant[C (Kmol)$^{-1}$]
R	universal gas constant[atm (kmol K)$^{-1}$]
$\xi_1, \xi_2, \xi_3, \xi_4$	fuel cell parameters
J_{max}	fuel cell maximum current density[A cm^{-2}]
J	fuel cell actual current density[A cm^{-2}]
T	absolute temperature[K]
A	constant dependent on the cell type[V]

The relationship between the flow of hydrogen through a valve and the partial pressure is given by [8]

$$\frac{q_{H_2}}{P_{H_2}} = \frac{K_{an}}{\sqrt{M_{H_2}}} = K_{H_2} \qquad (2.1)$$

The derivative of the partial pressure can be written as:

$$\frac{dP_{H_2}}{dt} = \frac{RT}{V_{an}}(q_{H_2}^{in} - q_{H_2}^{out} - q_{H_2}^{rea}) \tag{2.2}$$

The hydrogen flow rate reacted is calculated by

$$q_{H_2}^{rea} = N_0 I_{FC}/2F = 2K_r I_{FC} \tag{2.3}$$

Combine equations (2.1) (2.2) (2.3), and applying the Laplace transform, the hydrogen partial pressure can be rewritten with (2.4) and (2.5). Using similar techniques, oxygen partial pressure P_{O_2} can be obtained.

$$P_{H_2} = \frac{1/K_{H_2}}{1+\tau_{H_2}S}(q_{H_2}^{in} - 2K_r I_{FC}) \tag{2.4}$$

with

$$\tau_{H_2} = V_{an}/(K_{H_2}RT) \tag{2.5}$$

$$P_{O_2} = \frac{1/K_{O_2}}{1+\tau_{O_2}S}(q_{O_2}^{in} - 2K_r I_{FC}) \tag{2.6}$$

with

$$\tau_{O_2} = V_{ca}/(K_{O_2}RT) \tag{2.7}$$

The fuel cell voltage V_{cell} is less than its open circuit voltage E_{nernst} when current is drawn from the fuel cell stack. Activation polarization, Ohmic polarization and concentration polarization affect the whole overall polarization. The basic equations for the fuel cell voltage are as followed [8]:

$$V_{cell} = E_{nernst} - \eta_{act} - \eta_{ohmic} - \eta_{conc} \tag{2.8}$$

$$E_{nernst} = 1.229 - 0.85 \times 10^{-3}(T - 298.15) + 4.31 \times 10^{-5}T\ln(P_{H_2}P_{O_2}^{1/2}) \tag{2.9}$$

$$\eta_{act} = -[\xi_1 + \xi_2 T + \xi_3 T \times \ln(C_{O_2}) + \xi_4 T \times \ln(I_{FC})] \tag{2.10}$$

$$\eta_{ohmic} = I_{FC} \times (R_M + R_C) \tag{2.11}$$

$$\eta_{conc} = A \times \ln(1 - J / J_{max}) \tag{2.12}$$

The above equations including the dynamic gas transport model and the static polar model give rise to a fuel cell model, which can be used to generate voltage-current and power-current curves at different hydrogen flow rates under steady state as shown in Fig. 2-2. The rated power of the PEM fuel cell stack is 5kW and the nominal voltage is 33 V.
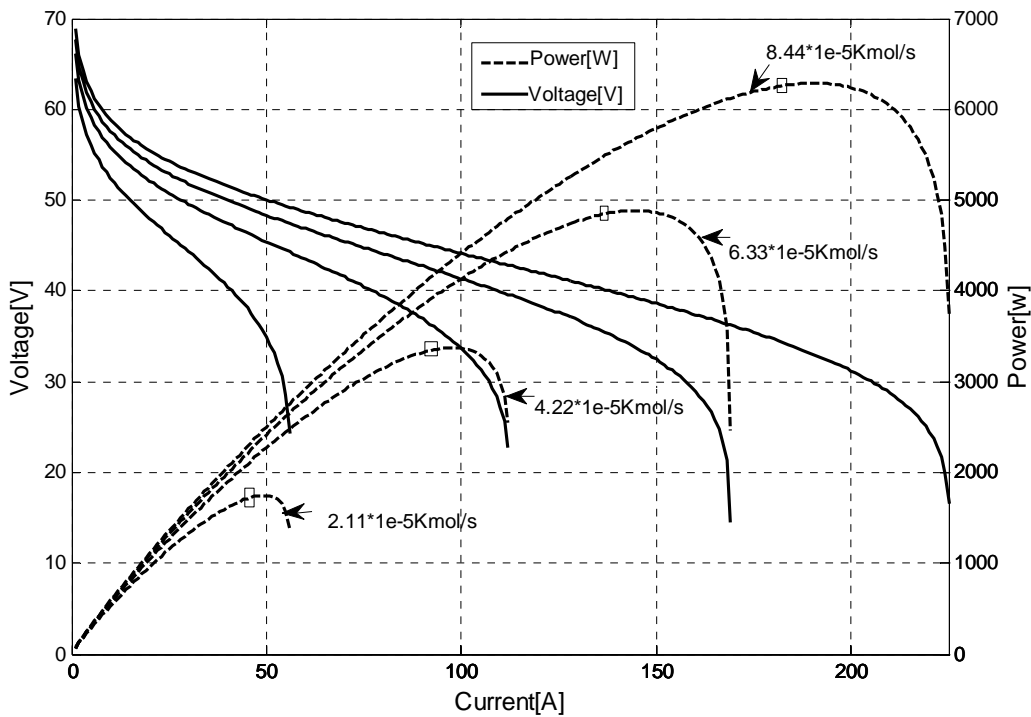
Figure 2-2: Fuel cell Voltage-current and power-current characteristics for different input hydrogen flow rates under steady state conditions.

From Figure 2-2, a mapping between fuel cell characteristic (minimum hydrogen flow rate, fuel cell current) and output power is implemented in a look up table with interpolation method shown in Table 2-1. For example, with a minimum hydrogen flow

rate of 6.33e-5 Kmol/s and a fuel cell current 137.75A, the fuel cell can generate a power of 4,859W, which is near to the maximum power point 4,886W for safety.

Applying this mapping inversely, specific output power of the fuel cell can be achieved by tuning the fuel flow rate with fuel cell reformer and adjusting the fuel cell current with booster converter according to the look up table.

Table 2-1: Mapping between fuel cell characteristics and output power.

Output power [W]	Input hydrogen flow rate [Kmol/s]	Fuel cell current [A]
6,251	8.44e-5	181.45
4,859	6.33e-5	137.75
3,354	4.22e-5	93.1
1,728	2.11e-5	46.55
0	0	0

2.3   FUEL REFORMER

After studying the complexity of the fuel processor due to complicated chemical reactions and considering its impact on the simulation time, a simplified model was adopted. The process concerned here is merely the time delays. This assumption is reasonable if the main objectives are system dynamic response, such as the power split between the fuel cell and the battery.

A second order transfer function was used to model the fuel reformer [10]:

$$\frac{q_{H_2}}{q_{methanem}} = \frac{CV}{\tau_1\tau_2 S^2 + (\tau_1 + \tau_2)S + 1} \tag{2-13}$$

where $q_{methanem}$ is Methane flow rate (Kmol s^{-1}); CV is the conversion rate from fuel to hydrogen, assumed to be 2; τ_1 and τ_2 are reformer time constants(s), set $\tau_1 = \tau_2 = 4$ to ensure that no unrealistic overshoot was present.
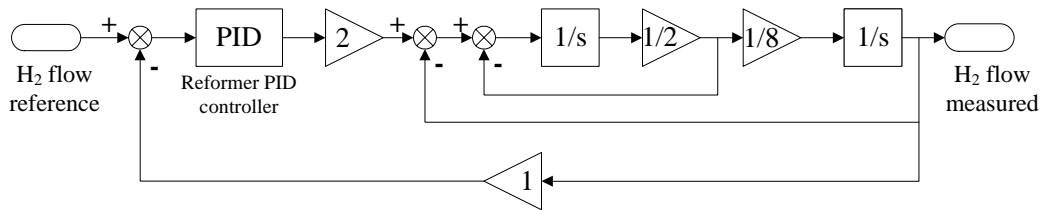
Figure 2-3: Reformer PID control system equivalent diagram.

The reformer PID controller was designed based on the equivalent diagram shown in Figure 2-3.

8

2.4 DC/DC CONVERTER

A DC/DC converter is the interface between the low voltage fuel cell stack and the higher voltage battery. The boost converter consists of inductor L, an IGBT switch, a diode, and the output filter capacitor, as shown in Figure 2-4.
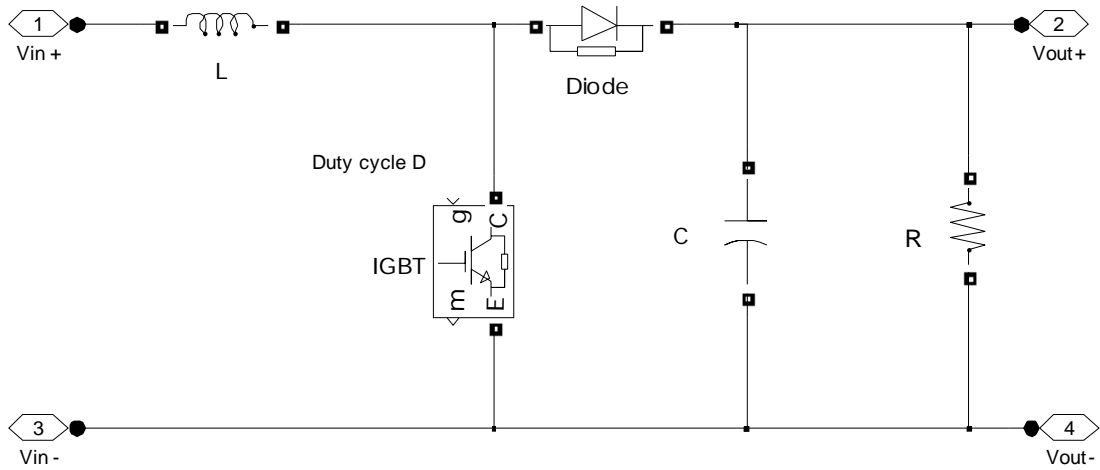
Figure 2-4: Classic boost DC/DC converter model.

For this work we selected the capacitor's voltage v_C and the inductor's current i_L as state variables. The small-signal model of a booster operating in continuous conduction mode (CCM) neglecting the parasitic parameters are:

$$\frac{d}{dt}\begin{bmatrix} \hat{i}_L(t) \\ \hat{v}_C(t) \end{bmatrix} = \begin{bmatrix} 0 & -\dfrac{1-D}{L} \\ \dfrac{1-D}{C} & -\dfrac{1}{RC} \end{bmatrix} \bullet \begin{bmatrix} \hat{i}_L(t) \\ \hat{v}_C(t) \end{bmatrix} + \begin{bmatrix} \dfrac{V_c}{L} \\ -\dfrac{I_L}{L} \end{bmatrix} \bullet \hat{d} \qquad (2\text{-}14)$$

$$y = \begin{bmatrix} 1 & 0 \end{bmatrix} \bullet \begin{bmatrix} \hat{i}_L(t) \\ \hat{v}_C(t) \end{bmatrix} \qquad (2\text{-}15)$$

Where D is the nominal duty cycle, V_c is the nominal output voltage of the converter, I_L is the nominal current through the inductor.

The duty cycle for the inductor current transfer function can be written as [11]

$$G_{id}(s) = \frac{\hat{i}_L(s)}{\hat{d}(s)} = \frac{V_c RCs + V_c + RI_L(1-D)}{RLCs^2 + Ls + R(1-D)^2}$$

(2-16)

In this work we selected a one-zero two-pole PI compensator (add integrator to increase the dc gain of C_i, and we added a zero to guarantee the closed loop has the expected bandwidth, and that the pole restrained the high frequency switch noise) as:

$$C_i = k \frac{w_i(1+\dfrac{s}{w_z})}{s(1+\dfrac{s}{w_p})}$$

(2-17)

Where w_i, w_z, w_p are the parameters of the PI compensator.

Based on this design, the crossover frequency of the current loop is 10^4 rad/sec. The phase margin is $61°$ (see Figure 2-5).
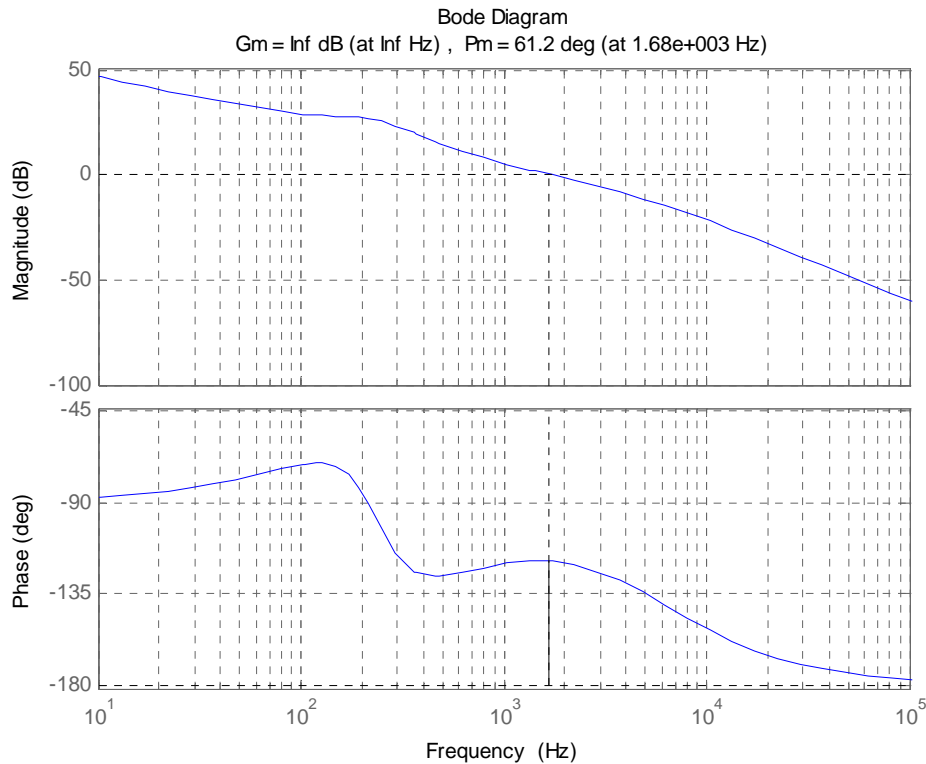
Figure 2-5: Compensated current loop Bode plot of the DC/DC booster.

DC/DC converters are time varying and nonlinear systems. In order to apply classic PID control theory, the small signal model was derived by linearization around a nominal point based on the average state model. The design based on the small signal model is easy to implement. However, the system is sensitive to the large variation of circuit parameters or large signal transients. In the denominator of the inductor current to duty cycle transfer function, there are four variables: L and C are the circuit parameters; R is the load information; while D is the nominal duty cycle. Any one of these can vary and lead to an instability of the system. During the sudden change of the load, the duty cycle D varies greatly. In this case, classic PID control theory is not effective. In that case, additional investigations would be required to develop an alternative method which is

11

robust against uncertain system parameters and sudden load changes. Sliding mode control techniques may be a possible solution to control the boost circuit [12].

2.5 BATTERY

Several methods have been used to estimate the state of charge (SOC) [13, 14].

Charge counting is one of the commonly used methods. The time integral of the measured current and the initial SOC provide a direct indication of the SOC. However, due to reliance on integration, noise errors in measurements are cumulative and lead to large SOC estimation errors.

Artificial neural networks (ANN) have been applied to estimate SOC. The primary advantage of the ANN method is that the initial SOC doesn't need to be known exactly before estimating the SOC. However, implementation of the ANN method needs a large number of training data and the training process can be relatively time consuming.

Another SOC estimation method involves measuring the battery's impedance over a wide range of ac frequencies at different states of charge. Values of the battery parameters can be found by data fitting. SOC can be estimated indirectly by correlating measured battery impedance with known impedance at various SOC levels. However, the impedance measurement by injecting signals into the battery is not applicable in real time.

In this paper, we choose the extended kalman filter method. The advantage of such methods is that the SOC can be estimated optimally in the presence of a Gaussian noise contained within the system bandwidth. In addition, the EKF based method does not need the precise information of initial SOC.
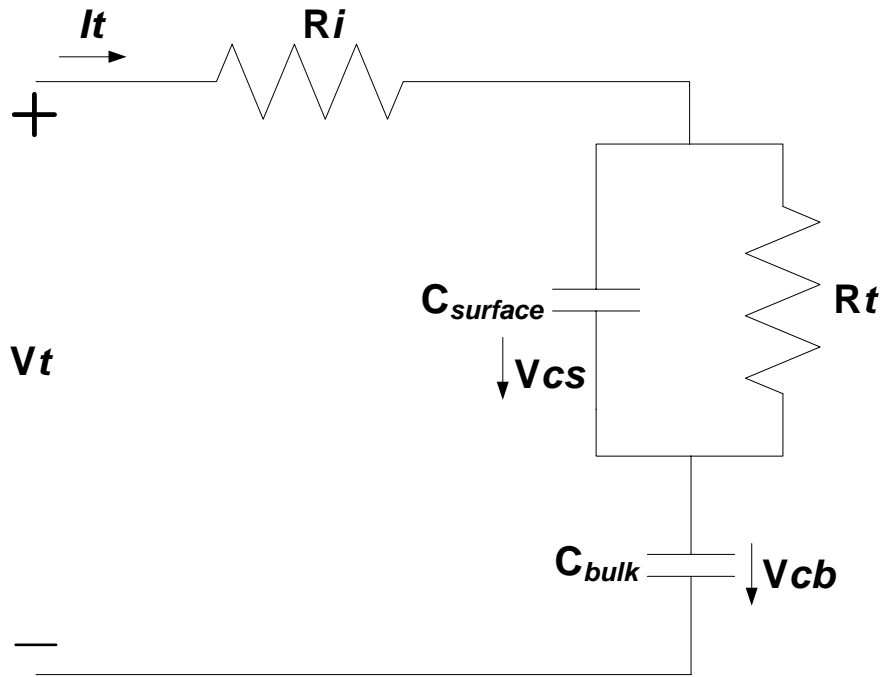
Figure 2-6: Equivalent circuit model of a lead acid battery.

The equivalent circuit model of a lead acid battery is shown in Figure 2-6. The terminal voltage and current is characterized by V_t and I_t. R_i is the internal resistance. A double layer capacitance $C_{surface}$ is in parallel with the charge transfer polarization represented by R_t. The voltage on C_{bulk} represents the open circuit voltage. The voltage across $C_{surface}$ and C_{bulk} are denoted by V_{cs} and V_{cb}.

The model used here assumes that the battery state of charge (SOC) and open circuit voltage have the following linear relationship

$$V_t = k \cdot SOC + d \tag{2-18}$$

where k and d are variables changing with SOC.

The state space model of the battery is

$$\dot{x} = f(x, u) + w \tag{2-19}$$

$$y = g(x,u) + v \tag{2-20}$$

Where $x = [SOC, V_{cs}]^T$, $y = V_t$, $u = I_t$, w and v process noise and measurement noise. The functions $f(x,u)$ and $g(x,u)$ are defined in equation (2-21) and (2-22) respectively.

$$f(x,u) = \begin{bmatrix} \dfrac{u}{k \cdot C_{cb}} \\[2mm] -\dfrac{x_2}{R_t \cdot C_{surface}} + \dfrac{u}{C_{surface}} \end{bmatrix} \tag{2-21}$$

$$g(x,u) = k \cdot x_1 + x_2 + R_i \cdot u + d \tag{2-22}$$

If we linearize the above equations by a first order Taylor-series expansion, the state space model with discrete time T_c is deduced in reference [13]

$$x_{k+1} = A_d \cdot x_k + B_d \cdot u_k = \begin{bmatrix} 1 & 0 \\[2mm] 0 & 1 - \dfrac{T_c}{R_t \cdot C_{surface}} \end{bmatrix} \cdot x_k + \begin{bmatrix} \dfrac{1}{k \cdot C_{cb}} \\[2mm] \dfrac{1}{C_{surface}} \end{bmatrix} \cdot u_k \tag{2-23}$$

$$y_{k+1} = C_d \cdot x_k + D_d \cdot u_k = \begin{bmatrix} k & 1 \end{bmatrix} \cdot x_k + R_i \cdot u_k \tag{2-24}$$

The algorithm of the extended kalman filter is executed as follows [13, 14]:

(1) Calculate the kalman gain

$$K_k = P_k C_k^T (C_k P_k C_k^T + R_w) \tag{2-25}$$

(2) Update estimate measurement

$$\hat{x}_{k+1} = f(\hat{x}_{k+1}, u_k) + K_k [y_k - g(\hat{x}_k, u_k)] \tag{2-26}$$

(3) Update error covariance measurement

$$P_{k+1} = A_k (E - K_k C_k) P_k A_k^T + Q_v \tag{2-27}$$

Where R_w and Q_v are process noise and measurement noise variance. P is the

covariance matrix, E is the unit matrix, $C_k \approx C_d$. $A_k \approx (A_d - E)/T_C$

In this way, Even though data from the battery sensor system contains Gaussian noise, the EKF can be used to estimate the SOC correctly from the terminal voltage measurement.

Figure 2-7, 2-8 and 2-9 show the results when measurement noise has zero mean with a standard deviation of 0.5V, 2V, and 20V respectively. We can see that, when the measurement noise is very large, the EKF gives SOC estimation that is nearly worthless. This is not a limitation of the EKF but results from the limitation of how much information we can derive from a certain noisy system.
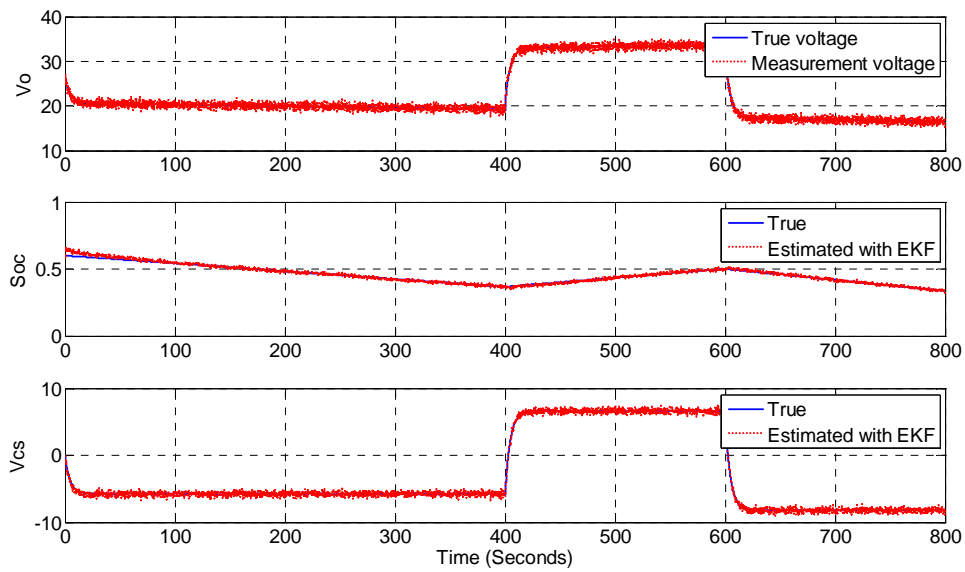
Figure 2-7: SOC estimation with measurement noise standard deviation =0.5V.
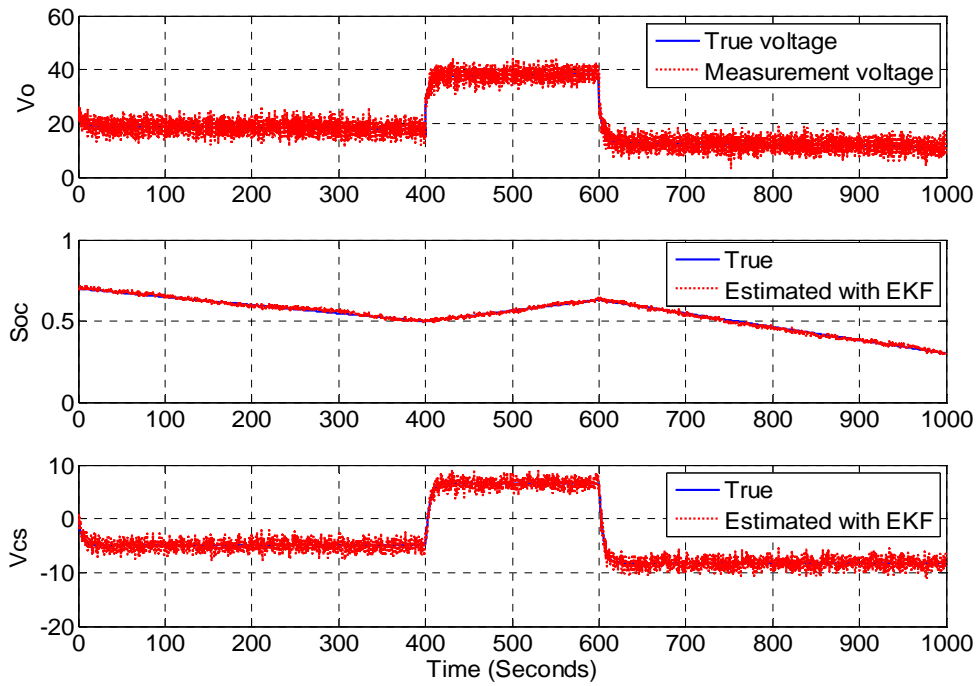
Figure 2-8: SOC estimation with measurement noise standard deviation =2V.
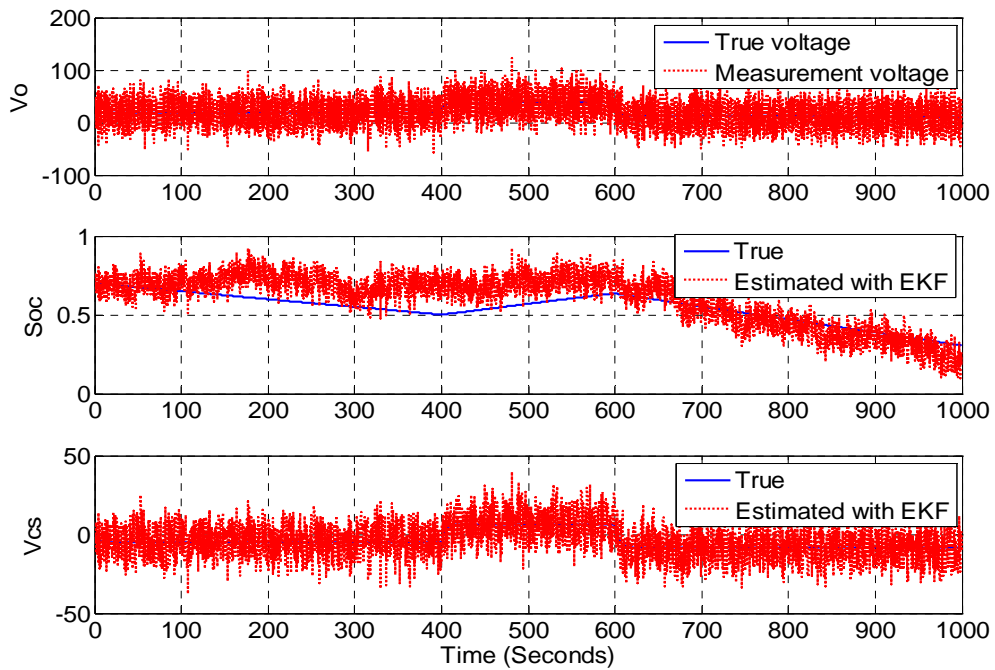
Figure 2-9: SOC estimation with measurement noise standard deviation =20V.

2.6 INVERTER

Figure 2-10 shows the typical model of a single phase full bridge DC/AC inverter with filter which is readily available in Matlab. Choose the capacitor's voltage u_o and the inductor's current i_L as state variables. The state space model of inverter is:

$$\frac{d}{dt}\begin{bmatrix} u_o \\ i_L \end{bmatrix} = \begin{bmatrix} 0 & -\dfrac{1}{C} \\ -\dfrac{1}{L} & -\dfrac{r}{L} \end{bmatrix} \bullet \begin{bmatrix} u_o \\ i_L \end{bmatrix} + \begin{bmatrix} 0 \\ -\dfrac{1}{L} \end{bmatrix} \bullet u_1 + \begin{bmatrix} -\dfrac{1}{C} \\ 0 \end{bmatrix} \bullet i_o \tag{2-28}$$

$$y = \begin{bmatrix} 1 & 0 \end{bmatrix} \bullet \begin{bmatrix} u_o \\ i_L \end{bmatrix} \tag{2-29}$$
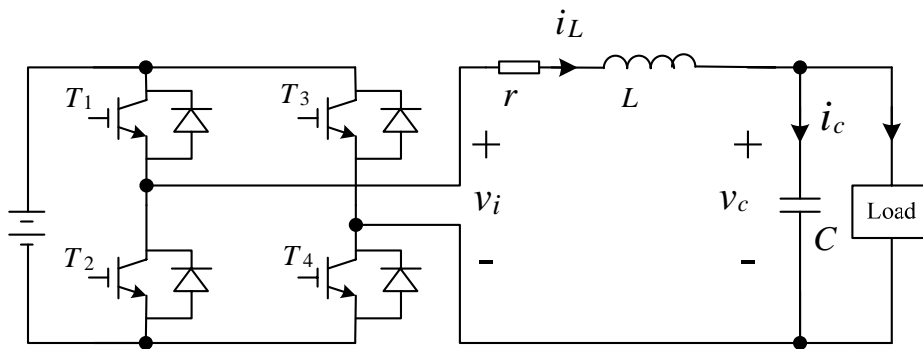
Figure 2-10: Classic model of single phase full bridge DC/AC inverter.

In order to maintain the load voltage and minimize the disturbances caused by the load transient, the inverter PID control system equivalent diagram designed is shown in Figure 2-11. The closed-loop transfer function about the input and output can be seen in equation (2-32).
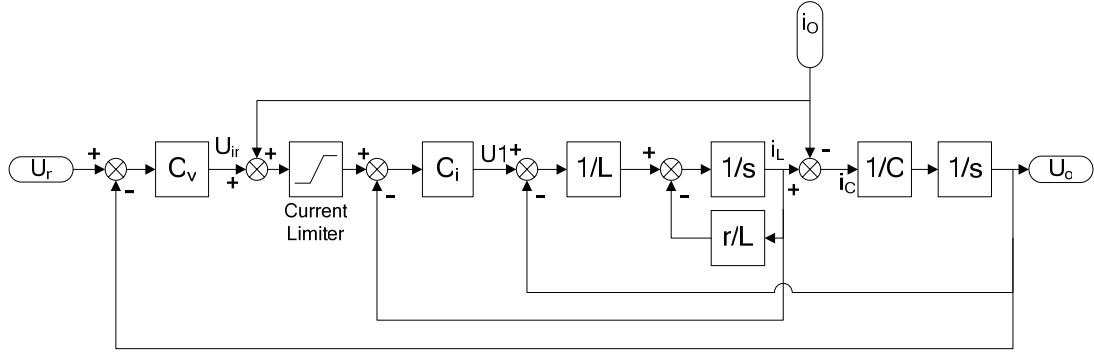
Figure 2-11: Inverter PID control system equivalent diagram.

Two PI compensators ($C_v \& C_i$) are used for the inner inductor's current loop and the outer capacitor's voltage loop. A load current feed-forward branch is added in order to improve the dynamic response and stability of the inner current loop. In addition, a current limiter is applied in the inner current loop to avoid excessive current [15].

$$C_v = k_{1p} + \frac{k_{1i}}{s} \tag{2-30}$$

$$C_i = k_{2p} + \frac{k_{2i}}{s} \tag{2-31}$$

$$U_o(s) = \frac{\dfrac{1}{LC}(k_{1p}s + k_{1i})(k_{2p}s + k_{2i})}{s^4 + \dfrac{Cr + Ck_{2p}}{LC}s^3 + \dfrac{1 + k_{1p}k_{2p} + Ck_{2i}}{LC} + \dfrac{k_{1p}k_{2i} + k_{2p}k_{1i}}{LC} + \dfrac{k_{1i}k_{2i}}{LC}} U_r(s)$$
$$- \frac{\dfrac{1}{LC}s^2(sL + r)}{s^4 + \dfrac{Cr + Ck_{2p}}{LC}s^3 + \dfrac{1 + k_{1p}k_{2p} + Ck_{2i}}{LC} + \dfrac{k_{1p}k_{2i} + k_{2p}k_{1i}}{LC} + \dfrac{k_{1i}k_{2i}}{LC}} I_o(s)$$

$$\tag{2-32}$$

The characteristic equation, whose roots are the poles of the closed-loop transfer function, is

19

$$D(S) = s^4 + \frac{Cr + Ck_{2p}}{LC} s^3 + \frac{1 + k_{1p}k_{2p} + Ck_{2i}}{LC} + \frac{k_{1p}k_{2i} + k_{2p}k_{1i}}{LC} + \frac{k_{1i}k_{2i}}{LC} \quad (2\text{-}33)$$

$$= (s^2 + 2\xi_r w_r + w_r^2)(s + m\xi_r w_r)(s + n\xi_r w_r)$$

By the pole assignment method, the parameters of C_v and C_i can be designed. The phase margin is $133°$ at 589Hz (see Figure 2-12).

Figure 2-12: Compensated outer voltage loop Bode plot for the inverter.

2.7   FUZZY LOGIC CONTROLLER

Fuzzy logic controller is a map from the controller inputs to outputs with a set of rules characterized by "if...then" statement. The if-part of the rules refers to adjectives that describe regions of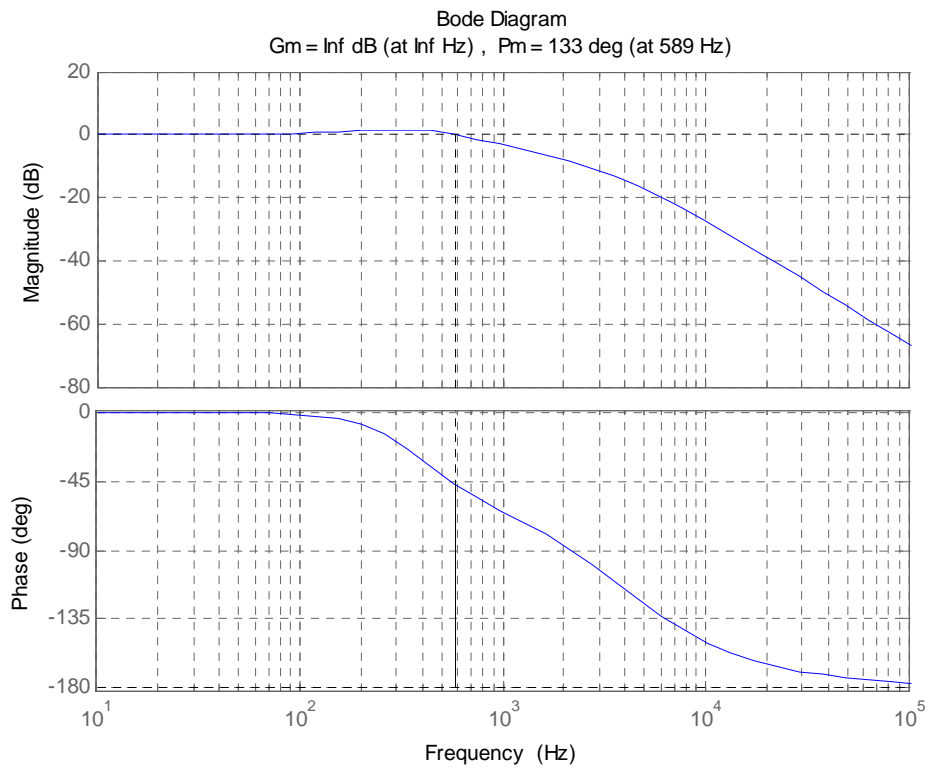 the input variables. Specific input value belongs to corresponding regions to a certain degree, which is represented by the degree of membership function. To obtain the output, the degrees of membership of the if-parts of all rules are evaluated, and the then-parts of all rules are averaged and weighted by the degrees of membership [16].

Limited by the inherent characteristics, fuel cells have a poor response to transient power demands due to chemical process delay. To mitigate the fuel cell from fatigue damage and smooth the fuel cell's operating conditions, a low pass filter is added before the raw load power signal is sent to the fuzzy logic controller. In this case, steady state load power is supplied by the fuel cell while the remaining transient load power is supplied by the battery automatically. The model uses the average load power as one of the input of the fuzzy logic controller. Another input is the estimated battery's SOC. The output of the fuzzy logic controller is the fuel cell output power. The designed FLC will let the fuel cells supply steady state power while keep SOC around the desire value of 0.6.

The procedure for creating the fuzzy logic controller is as follows:

(1)   Define the first input variable as the estimated battery SOC. The input range is 0 to 1. Five patterns are sorted including following:

     (a)   VL: represents a very low SOC, the range is 0-0.55;

     (b)   L: represents a low SOC, the range is 0.4-0.6;

     (c)   M: represent a medium SOC, the range is 0.55-0.65;

(d)   H: represent a high SOC, the range is 0.6-0.8;

(e)   VH: represent a very high SOC, the range is 0.65-1.

(2)   Define the second input variable as the average active load power. The input range is 0 to 1. Three patterns are sorted including following:

(a)   L: represents a low average load power and the range is 0-0.5;

(b)   M: represent a medium average load power and the range is 0.1-0.9;

(c)   H: represent a high average load power and the range is 0.5-1.

(3)   Define the output variable as the fuel cell output power. The input range is 0 to 1. Four patterns are sorted including following:

(a)   L: represents a low fuel cell output power and the range is 0-0.35;

(b)   M: represent a medium fuel cell output power and the range is 0.1-0.6;

(c)   H: represent a high fuel cell output power and the range is 0.35-0.85;

(d)   VH: represent a very high fuel cell output power and the range is 0.6-1.

(4)   Then use Fuzzy inference ''IF Input1 IS … AND Input2 IS … THEN Output IS …'' to determine the Fuzzy rule. For example:

(a)   If SOC is very high, then fuel cell output power is low;

(b)   If SOC is medium and filtered load power is low, then fuel cell output power is high;

(c)   If SOC is medium and filtered load power is medium, then fuel cell output power is medium;

(d)   If SOC is low and filtered load power is low, then fuel cell output power is medium.

…..etc.

Figure 2-13 shows the fuzzy inference system. It displays a high level diagram of the designed fuzzy logic controller. Inputs and their membership functions appear to the left, while outputs and their membership functions appear on the right. Figure 2-14 shows the membership function of inputs and outputs. Table 2-2 shows the fuzzy logic rules. Fig. 2-15 shows the result of the fuzzy logic controller.

Figure 2-13: Fuzzy inference system.
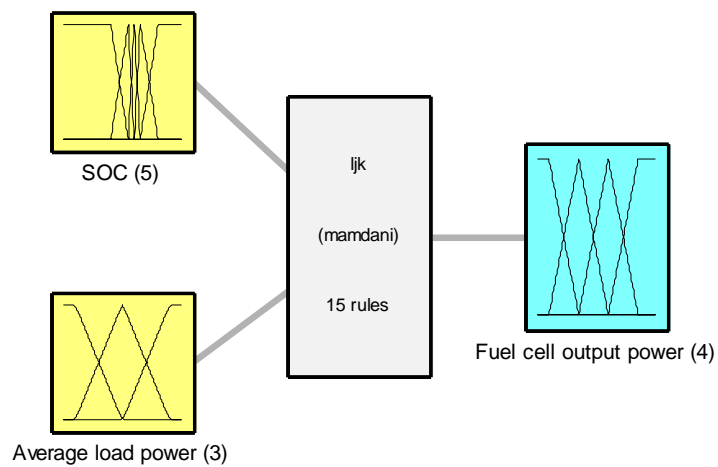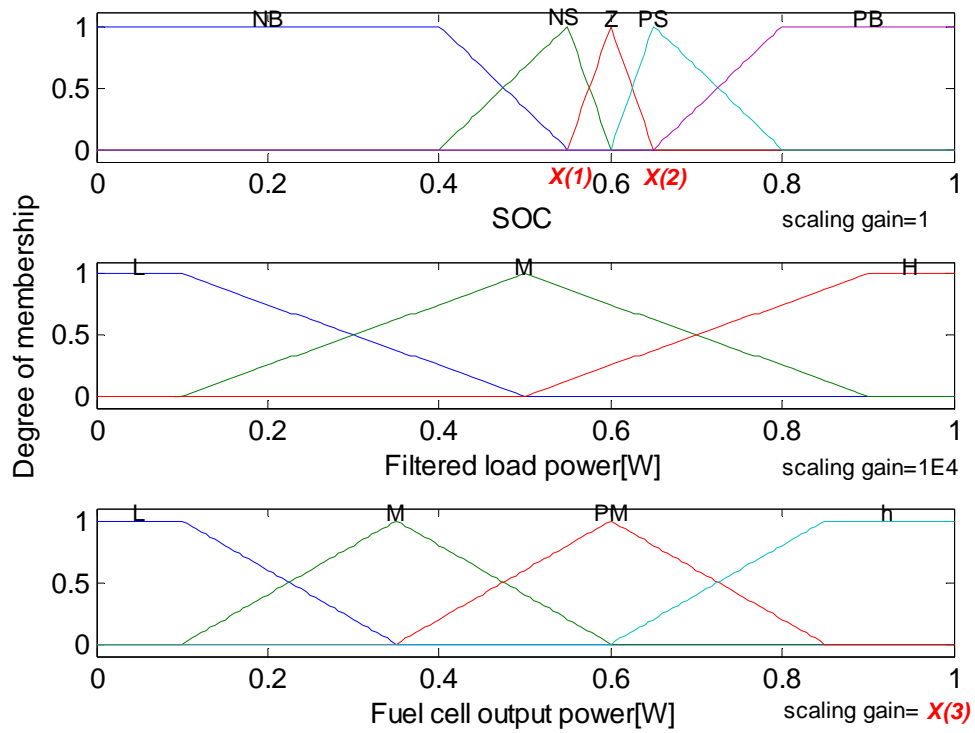
Figure 2-14: Membership functions of input and output variables.
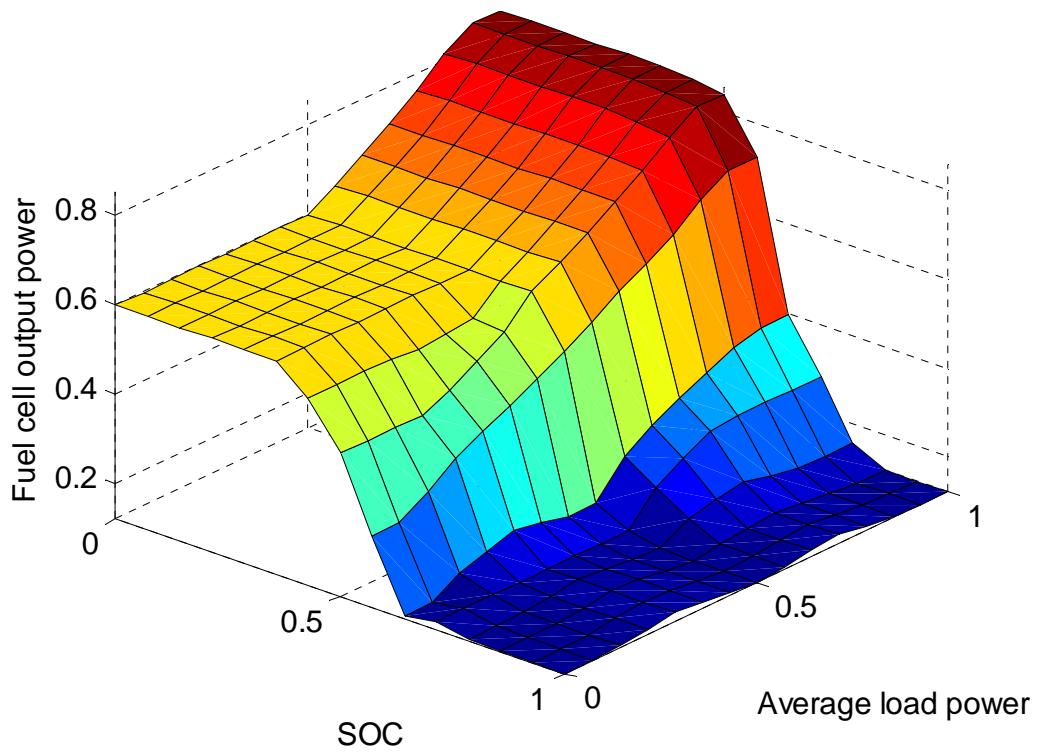
Figure 2-15: Output result of fuzzy logic controller.

Table 2-2: Rule table for the fuzzy logic controller.

| Fuel cell | | Averaged load power | | |
Output power		L	M	H
SOC	VL	H	H	VH
	L	M	H	VH
	M	L	M	H
	H	L	L	M
	VH	L	L	L

25

2.8   GENETIC ALGORITHM

There are too many parameters (scaling gains, membership function shape and position, number and type of rules) that can be tuned to improve the performance of the designed fuzzy logic controller. However, to achieve the specific objectives, there is no direct and clear method to tune these parameters. Some basic design guidelines are as follows [17]:

Try tuning the fuzzy controller using the scaling gains;

Try adding or modify rules and membership function;

If chattering behavior occurs, you may have a gain set too high. Setting the input gain too high makes it so that the membership function saturate for very low value, which lead to oscillation;

Sometimes, adding more membership functions and rules may help. These can reduce chattering;

….

Here, we choose the genetic algorithm to find the suitable parameters efficiently as it can artificially tune the parameters and find a global optimum that meets the design objective.

CHAPTER 3 SIMULATION RESULTS

3.1   GA Based Optimal Fuzzy Logic Controller For Dc Load

To improve performance of the designed fuzzy logic controller, a genetic algorithm (GA) was used to find a global optimum that met the design objective.

The optimization object was to minimize the following fitness function during the whole simulation time.

$$J = \int (SOC - SOC_{ref})^2 \tag{3-1}$$

Where SOC_{ref} is equal to 0.6 at which the battery's internal resistance is least. This object will reduce the fluctuation and extend the lifetime of the battery.

The tuning parameter related to this object involves scaling gains, membership function (MF) shape and the number and type of rules. For simplicity, only three tune parameters listed in Table 3-1 were considered. Setting the upper and lower bound for each parameter helps the GA search for the optimum solution efficiently [17].

Table 3-1: Tuning parameters with lower and upper bounds

Tuning parameter	Bounds
X(1): Left corner of 'Z' MF of input variable "SOC"	[0.4,0.6]
X(2): Right corner of 'Z' MF of input variable "SOC"	[0.6,0.8]
X(3):Scaling gain for output variable "fuel cell output power"	[6000,7500]

The scheme of the optimization process is show in Figure 3-1. The convergence criterion is chosen as whether the maximum number of generations reaches 20.
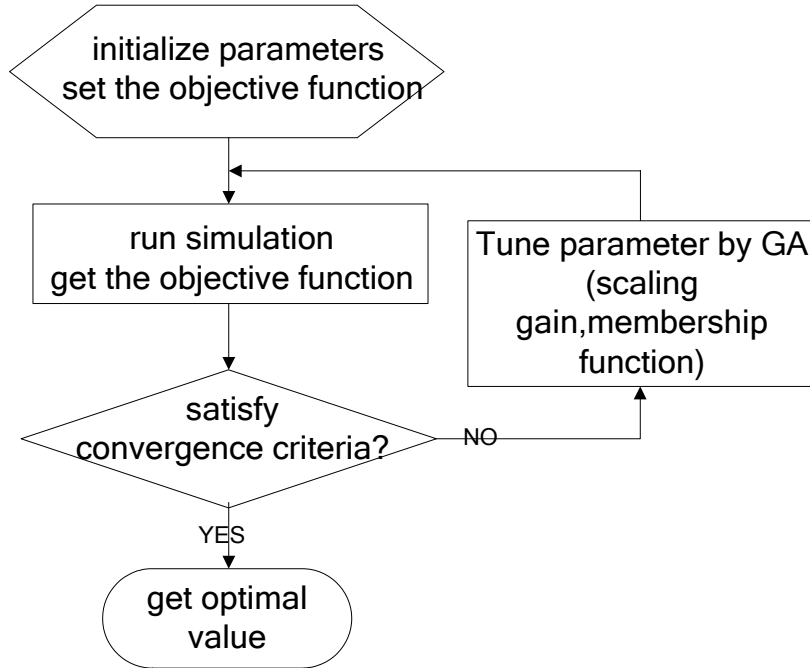
Figure 3-1: Scheme of the optimization process based on GA.

MATLAB® and Simulink® have been used to verify the validation of the proposed model and associated control strategies. In the simulation, the fuel cell output power is rated as 5kW and the maximum power is 6kW. The nominal voltage and capacity of the battery is 75V and 54Ah respectively. The whole running time is 600s.

Figure 3-2 shows the load profile for the time interval between 0 and 600s. This was used to test the dynamic response of the hybrid system. For the load profile shown, the optimal parameters found are listed in Table 3-2. Figure 3-3 shows the variation of fitness function at each generation. Obviously, the search for optimal parameters is convergence.

Table 3-2: Optimal parameters found by GA

X(1)	X(2)	X(3)	-J
0.575546	0.641195	7158.593	-0.89936

Figure 3-2: Average load power profile.
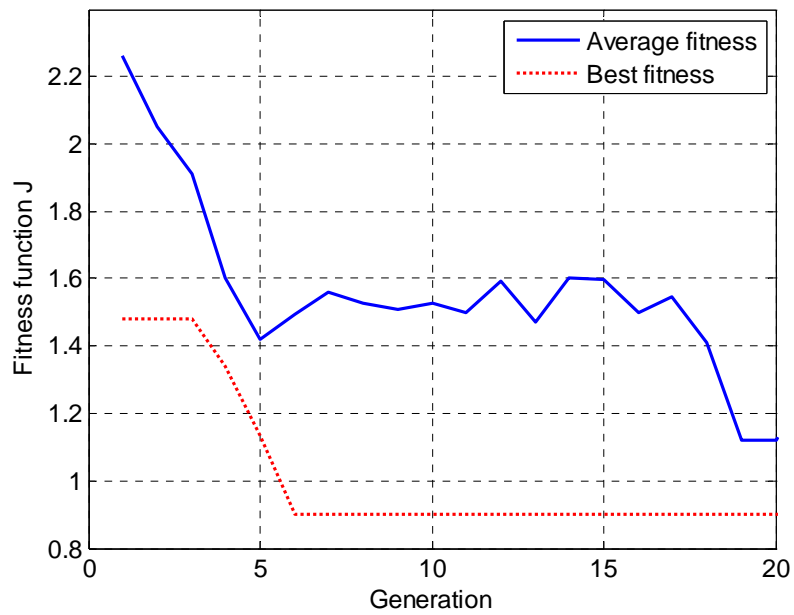
Figure 3-3: Fitness function value varies with the generation.

Figure 3-4 to Figure 3-7 show the dynamic response of the hybrid system based on the optimal parameters found by GA.

Figure 3-4 shows the load power shared by the fuel cell and battery. To meet the required load active power, the fuel cell provides a steady-state power for fuel cel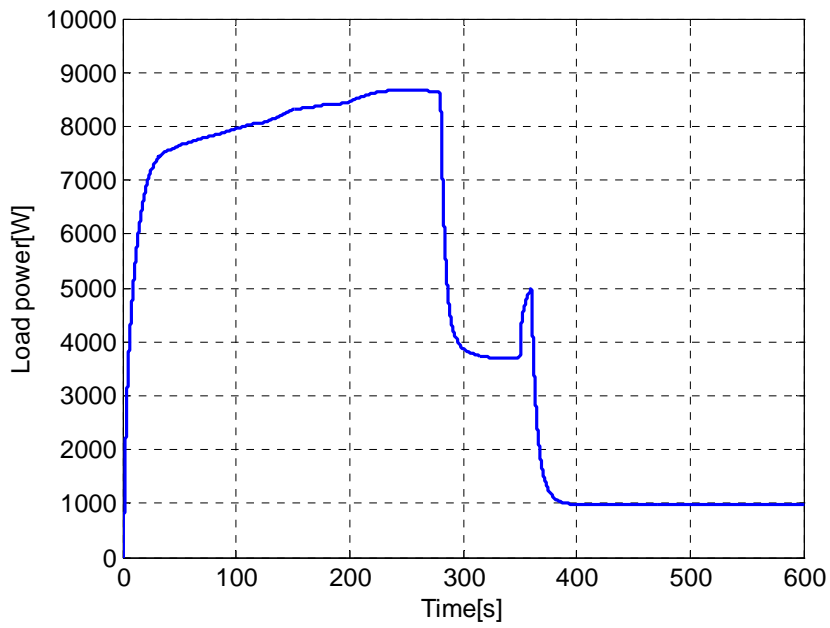l safety and durability while the battery provides most the remaining transient power automatically. This power split strategy makes the best use of the two power sources.
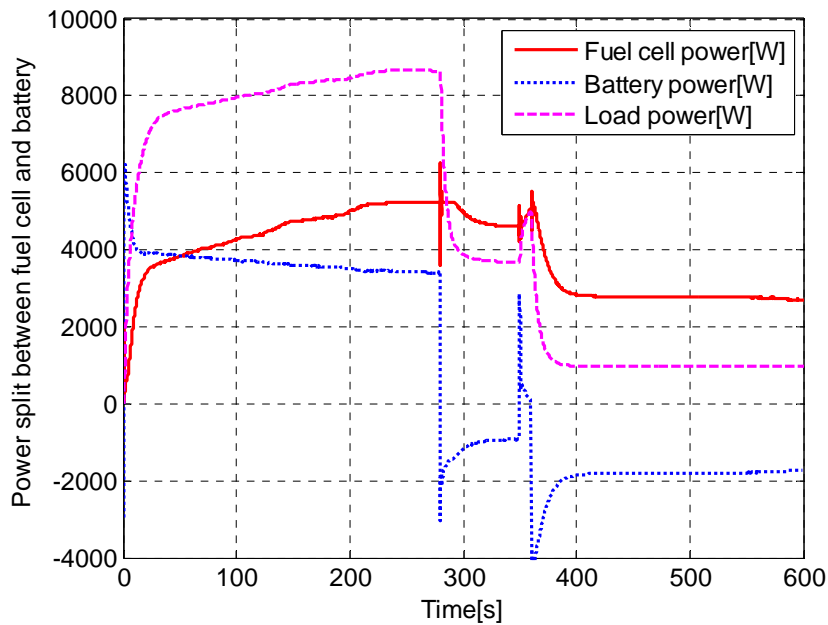
Figure 3-4: Power split between fuel and battery.

Figure 3-5 compares the estimated SOC by EKF with the actual value. From the figure, we can observe that, thanks to the combination of the correction and prediction process [13], the extended kalman filter gave a reasonable estimation of the SOC in the presence of the measurement noise. During the first few seconds, the battery provided most of the load power as the fuel cell needed time to start up. Then both the battery and the fuel cell supplied power to the load when the load power demand was high. The high discharging current dropped the SOC below 0.6. During the remaining 300s with lower power demanded, the power management controller commanded the fuel cell to provide more power than the load demanded to charge the battery. In this way, the battery SOC

steadily returns back towards the desire value.
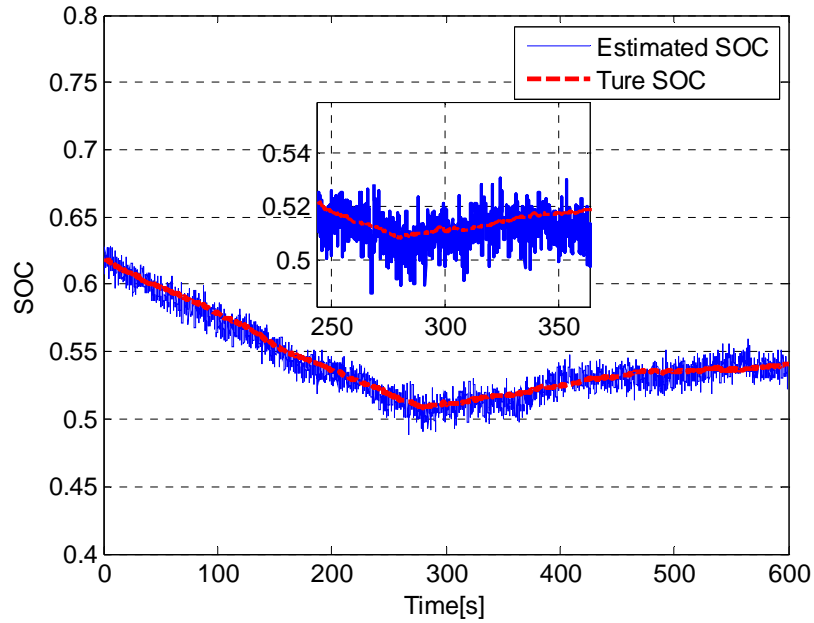
Figure 3-5: The variation of battery SOC.

Figure 3-6 shows transients associated with the battery voltage and current. The battery voltage varied significantly as large battery current caused certain voltage drop across the battery's internal resistance. During negative battery current the battery was charged by the fuel cell and positive battery current means the battery was discharging.

Figure 3-7 displays the variation of fuel cell voltage and current. The fuel cell voltage stayed within the acceptable range of 30 to 35 volts.
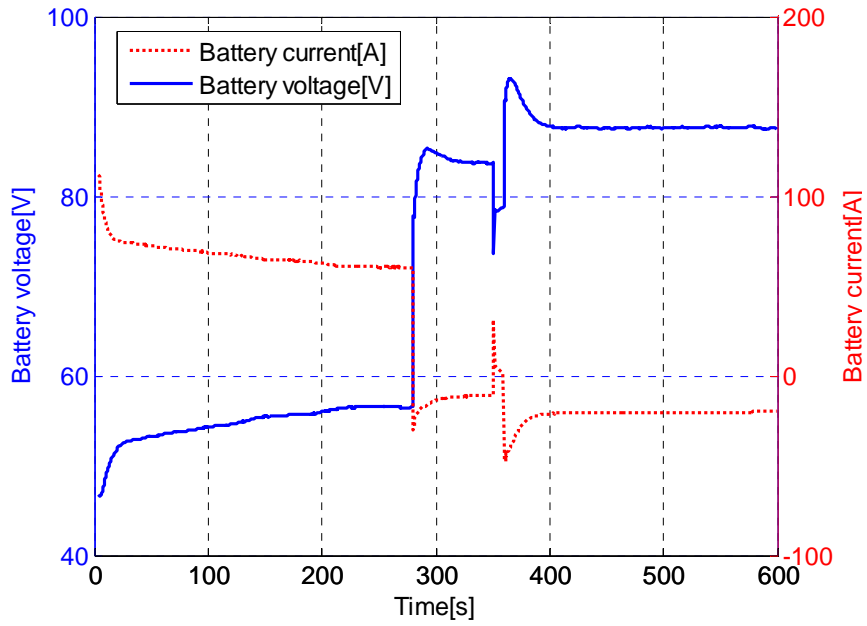
Figure 3-6: Variation of battery voltage and current during load transitions.
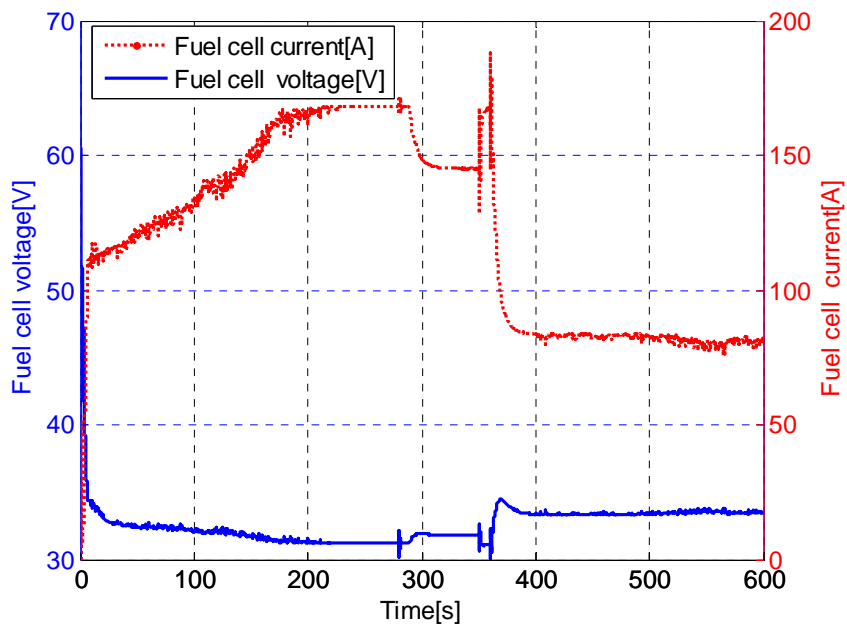
Figure 3-7: Variation of fuel cell voltage and current.

3.2 Fuzzy Logic Control For Ac Load

MATLAB® and Simulink® have been used to construct and study the model and associated control strategies. The running time for this load profile was 500s. The specifications of the hybrid system are shown in Table 3-3 in detail.

Table 3-3: Specifications of the hybrid system

| Simulation parameters in Matlab			
Start time	Stop time	Time step	Solver
0s	500s	2e-5s	ode1(Euler)
Fuel cell stack			
Type	No of fuel cells	Rated voltage	Rated current
PEM	65	36V	140A
Rated power	Hydrogen time constant	Oxygen time constant	Water time constant
5kW	3.37s	6.74s	18.418s
DC/DC converter			
Type	Rated input voltage	Rated input current	Rated output voltage
boost	30-50V	0-150A	200V
Capacitance	Inductor	Switch frequency	
400e-6C	20e-3H	20kHz	
Battery			
Type	No of module	Capacity	Rated voltage
Lead acid	24	432Ah	200V
Internal resistance	Initial state of charge	Double layer capacitance	Bulk capacitance
0.1174/module	0.62	27.31C/module	11252.4C/module
DC/AC inverter			
Voltage reference	DC input voltage	Switch frequency	Filter resistance
$110V_{RMS}$/60Hz	180-200V	10kHz	0.1ohm
Filter inductor	Filter capacitance		
0.43e-3H	140*1e-6C		
Load			
Load voltage	Maximum load active power	Maximum load reactive power	Power factor
$110V_{RMS}$/60Hz	10000W	6000Var	(-0.85,0.85)
Rated power	Rated Power factor		
5000W	0.85		

Figure 3-8 shows the load profile for the time interval between 0 and 500s which consists of a variety of active power and reactive power with different power factor. Some what arbitrarily, the load can be considered to consist of a washing machine, a microwave, a small transformer with secondary open circuited, and a capacitor bank. At time 50s, the reactive power step increase from 5,213W to 8,333W. At 200s, the reactive power steps down to 4,170W. During 297-300s, there exists a short time interruption required for 10kW power which is out of the capacity of the hybrid system. The load active power steps down to a low value around 1,000W after stepping up to 5,000W in the time interval 355-360s. This load profile with different load type and load transient will be used to test the dynamic response of the hybrid system.

Figure 3-9 shows the active power shared by the fuel cell and the battery. To meet the required load active power, the fuel cell provides a steady-state power for fuel cell safety and durability while the battery provided the remaining transient power automatically. This power split strategy makes the best use of the two power sources.
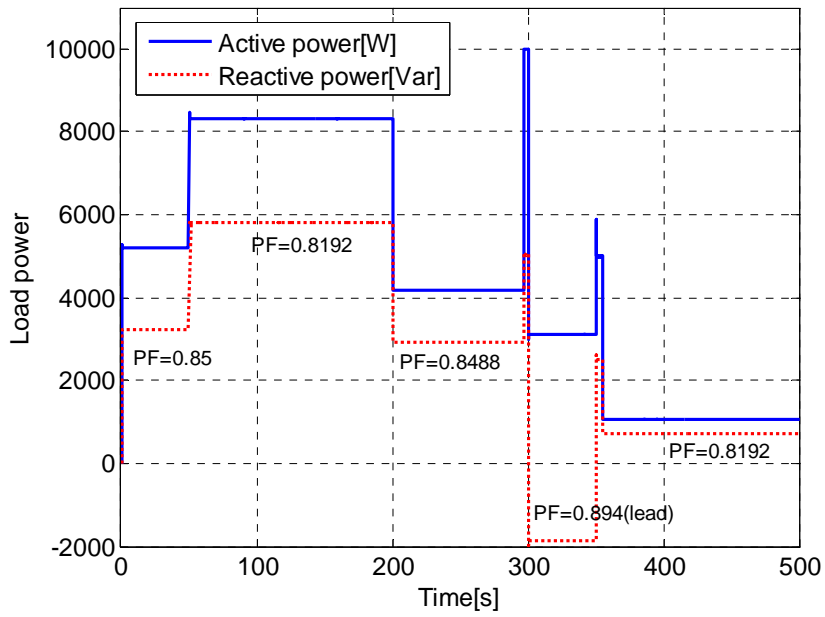
Figure 3-8: Average load power profile (calculated based on 60Hz).
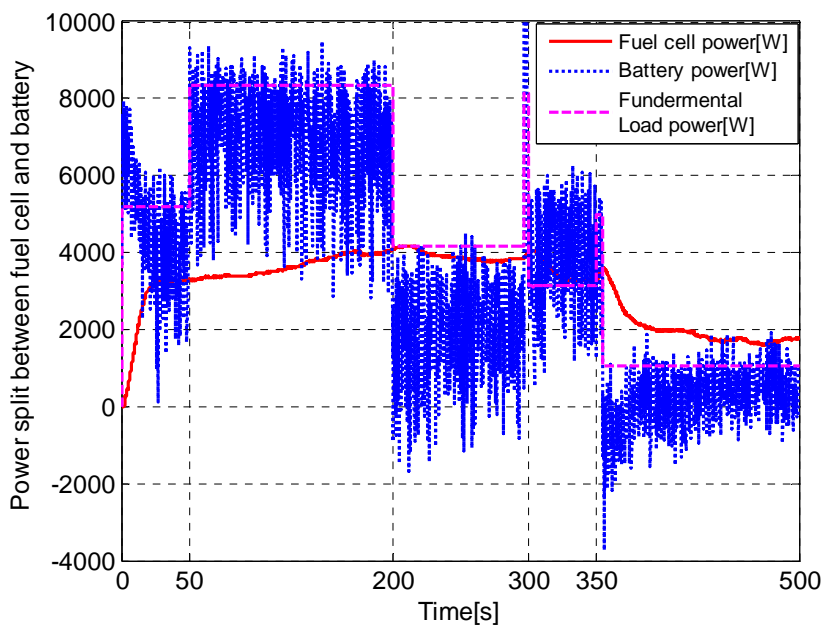
Figure 3-9: Power split between the fuel cell and the battery.

35
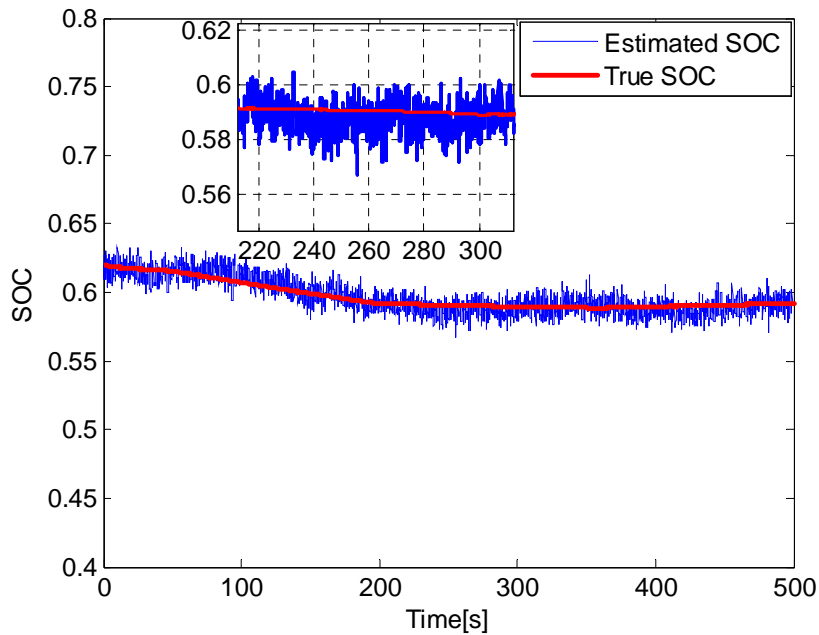
Figure 3-10: The variation of battery SOC.

Figure 3-10 compares the estimated SOC by EKF with the actual value. From the figure, we can observe that, thanks to the combination of correction and prediction process [13], the extended kalman filter gave a reasonable estimation of the SOC in the presence of measurement noise. During the first 200s, both the battery and the fuel cell supplied power to the load. Since the initial battery SOC was 0.62, a little higher than the desired value of 0.6, the power management controller let the battery provide most of the power to the load. The high discharging current dropped the SOC below 0.6. During the remaining 300s with lower load profile, the power management controller commanded the fuel cell to provide more power than required for the load to charge the battery. In this way, the battery SOC steadily returned back towards the desire value.

Figure 3-11 shows transients associated with the battery voltage and current. The battery voltage stays between180V and 220V which is in an acceptable range (10% for

36

200V nominal voltage). However, the battery terminal voltage varies significantly as large battery current causes voltage drop across the battery's internal resistance. As the input current of the inverter contains large harmonic component, the battery current fluctuated frequently. The negative battery current means the battery was being charged by the fuel cell and positive battery current means the battery was discharging.
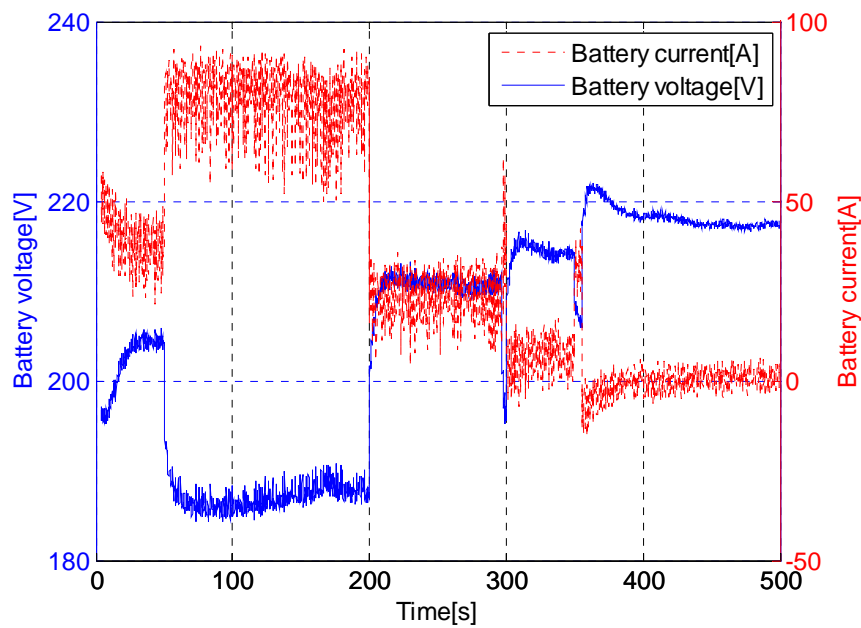
Figure 3-11: Transient of batter voltage and current.

Figure 3-12 illustrates how the actual hydrogen flow rate changes with the step load. It tracks the hydrogen flow rate command well but there exits some time delay due to the time constant of the reformer.

Figure 3-14 shows the load voltage and current during each load step. The RMS output voltage of the inverter stays constant as the load changes shown in figure 3-13, which proves that the inverter with the dual loop controller has good steady state and dynamic performance. During the short time interruption (297s-300s), the voltage and current wave distort, as the current limiter block in the inner current loop takes effect and

protects the whole system against excessive current. Large sampling times in the captured

data accounts for the stair step in the voltage waves in Figure 3-15, 3-16, 3-17, and 3-18.

A close-up view of the inverter output voltage and current, which are also the load

voltage and current, is shown in Figure 3-15, 3-16, 3-17, and 3-18.
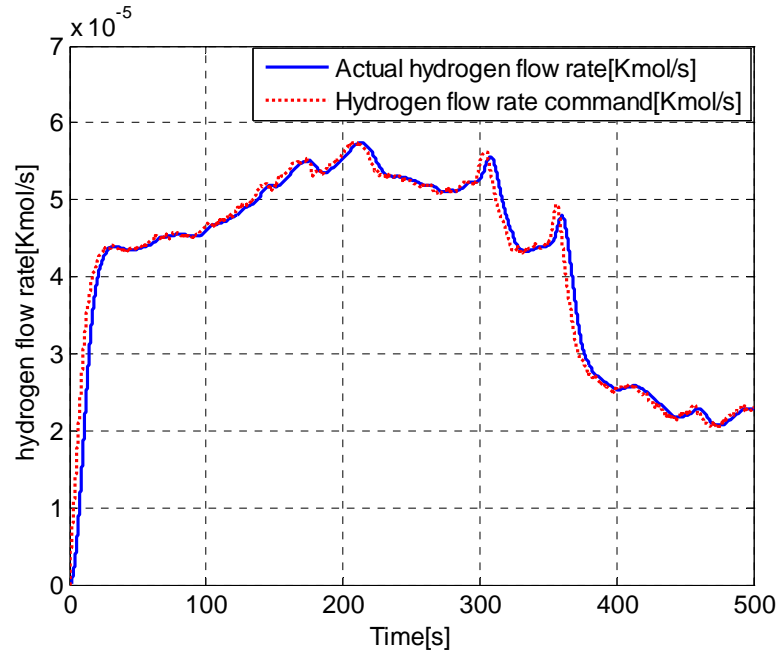
Figure 3-12: The variation of hydrogen flow rate feeding into fuel cell stack.

Figure 3-13: The variation of load voltage and current.

Figure 3-14: Load voltage and current at each load step point.
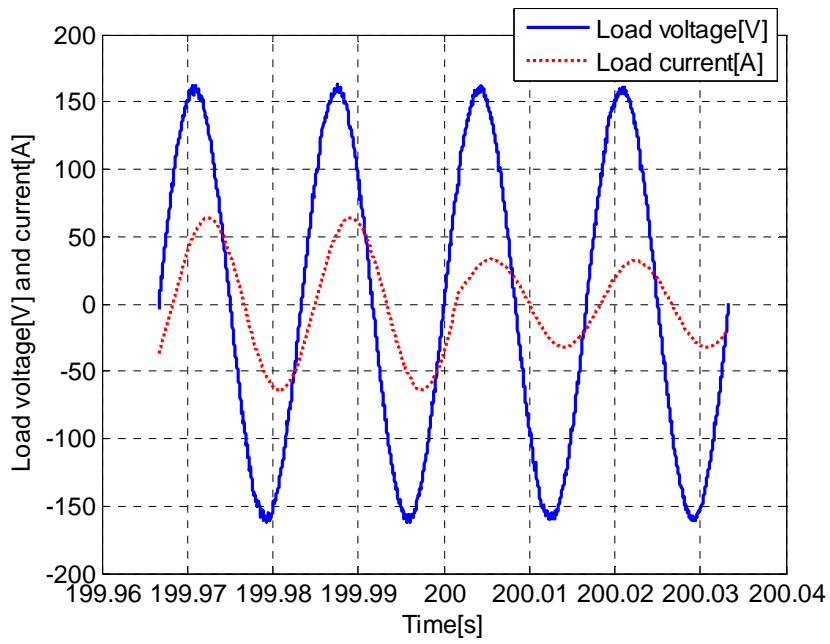
Figure 3-15: Inverter output waveform zoomed at t = 200s.
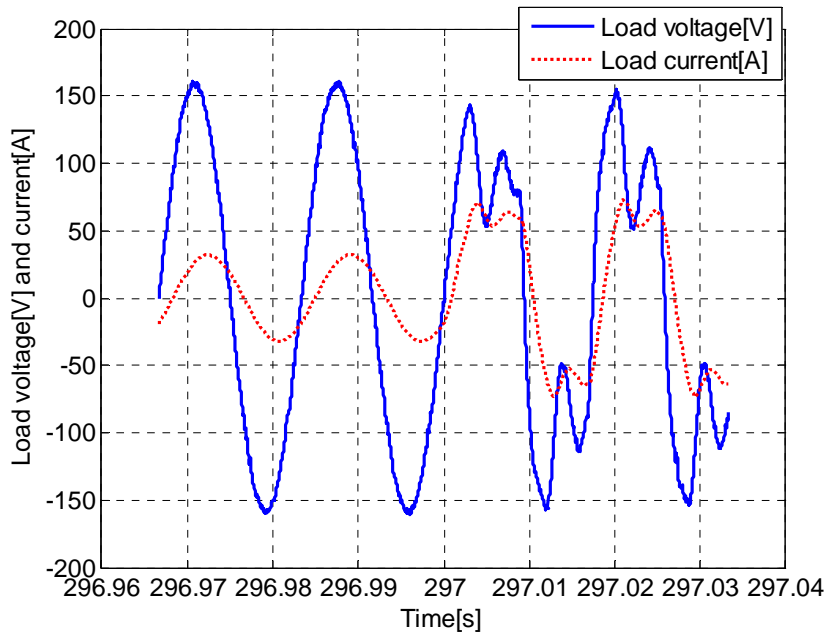
Figure 3-16: Inverter output waveform zoomed at t = 297s.
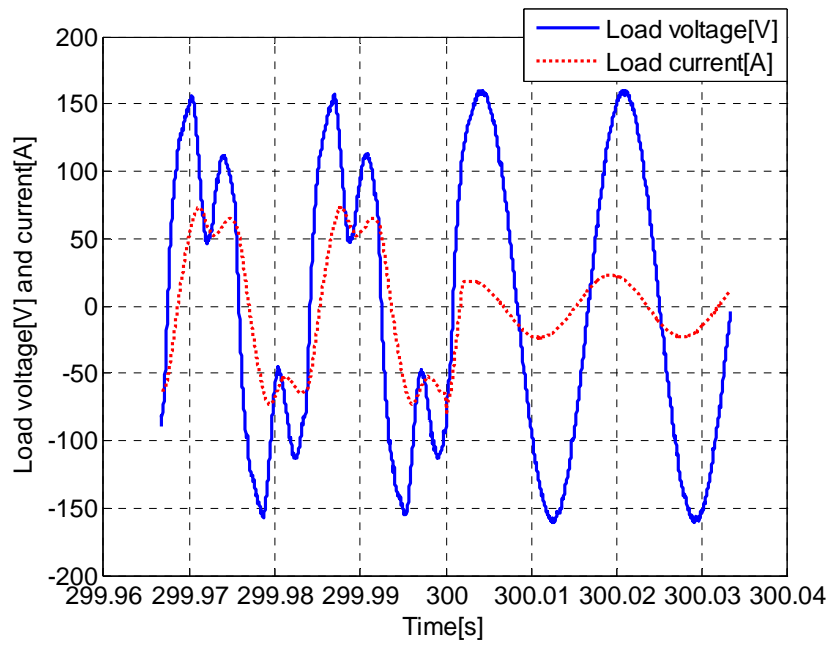
Figure 3-17: Inverter output waveform zoomed at t = 300s.
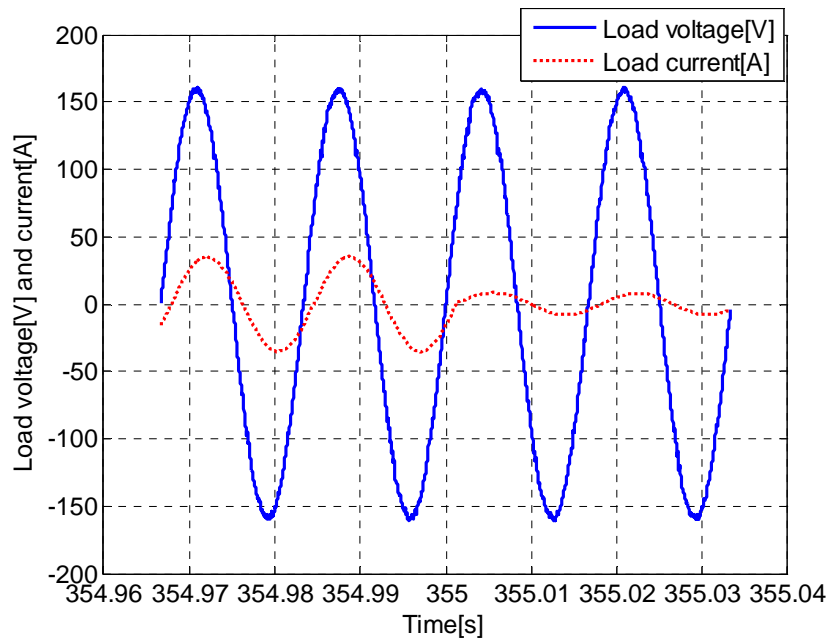
Figure 3-18: Inverter output waveform zoomed at t = 355s.

CHAPTER 4 DISCUSSION AND CONCLUSIONS

4.1 DISCUSSION

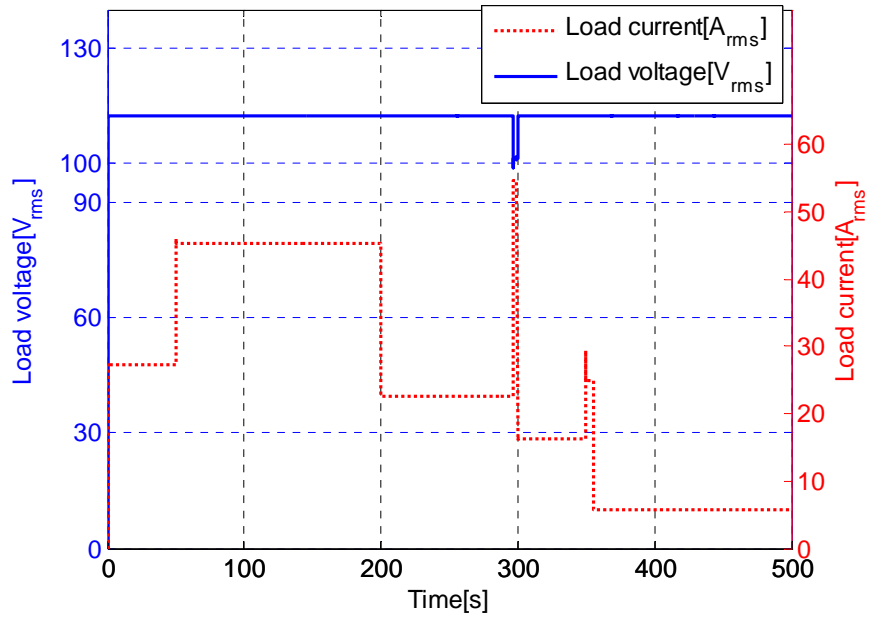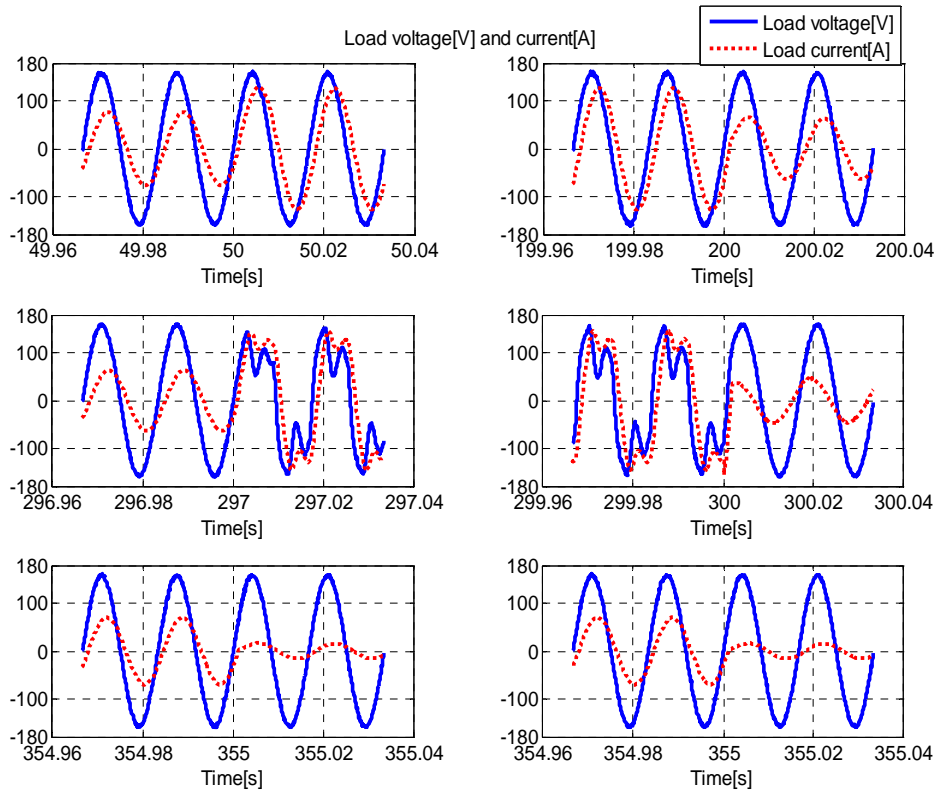The control on the power side has been fully developed including the control of DC/DC converter, DC/AC inverter, and power management based on the battery state of charge estimate. From the designed model, the followings things can be determined: the capacity of the fuel cell stack, restrictions due to the finite response time of the fuel processor, the specification of the battery size, and the classic circuit parameters of DC/DC converter and the DC/AC inverter. What's more, the setup of the whole system is modular and can be modified easily. Table 4-3 shows the specification of fuel cell stack and battery according to load power.

Table 4-1: Specification of fuel cell stack and battery according to load power

Fuel cell stack	Battery	Load power
65 cells, 2kW/40V	200V,144Ah	2kW
65 cells, 5kW/35V	200V,432Ah	5kW
65 cells, 10kW/33V	200V,864Ah	10kW

However, modeling and control of the fuel processor and the fuel cell stack have not yet been thoroughly considered.

(1) The controls for the process inside the fuel processor are not mentioned as we use a simplified fuel reformer model. The main control loops inside the fuel processor systems consists of the diesel supply to the burner, the air compressor, the water management and the cooling systems. In addition, the fuel reformer's feature of rapid cold start should be considered carefully as it affects the whole system's dynamic response;

(2) The fuel cell stack itself has a dynamic and nonlinear behavior and is sensitive

to variable changes, such as fluctuation of pressure, temperature and humidity. A controller needs to be developed to stabilize the stack operation even under adverse conditions. For example, when humidity is outside of accepted levels, what measures (increase cathode air, increase stack temperature, decrease stack current, etc.) should be taken to counteract this.

Furthermore, the following issues should be considered:

(1) The system model adopts the classic topology of the power electronics devices. Different topology may be considered to improve the system efficiency. In addition, different circuit parameters and load profiles may lead to instability of the controller. Advance control methods may be needed such as slide model control for the DC/DC converter;

(2) Complicating factors in the simulation include the extended computation time due to power electronic devices. This problem will worsen considerably when a detailed fuel processor model is incorporated in the system. A balance should be made to combine two different time constants. For example, to study the non-quasi-steady-state situations such as cold startups, the DC/AC inverter model should be simplified to speed up the simulation process in the Matlab environment. The simplified inverter model will not change the power management strategy as it is a relatively independent module. Unfortunately, the simplified inverter model will lose some valuable information, especially the harmonic content on the input side. The harmonic currents caused by the switches will cause large charging and discharging current into and out of the battery, thus affect the estimation of battery SOC;

(3) The objective of this work is to develop a hybrid system but not optimize

efficiency. The efficiency maps of each component need to be developed. These can be use to identify the optimum operating points of the hybrid system and to make the system cost efficient.

4.2 CONCLUSIONS

Dynamic modeling and control of each subsystem has not been fully considered. First, a more effective charge/discharge control strategy was not designed as an accurate state of charge estimation system was not developed. Secondly, the DC/AC converter was not included in the whole design or is simplified. The major feature of this study was presenting a comprehensive dynamic model including power electronic devices with associated control strategies. The primary target in the research was to operate the fuel cell near the maximum power point and keep the SOC of battery within an accepted range.

(1) A fuel cell characteristic look up table was built to operate the fuel cell near the maximum power point;

(2) An estimator method based on EKF was developed to estimate the battery SOC in the presence of measurement noise;

(3) A dual loop controller was designed for the single phase inverter to keep the load voltage constant;

(4) An optimal fuzzy logic method was used to design the power management controller. Simulation results show it can make the best use of the fuel cell and battery to meet the power demand of the load.

Future work will include:

(1) Optimize the power management controller using genetic algorithms that consider the efficiency and cost of the system;

(2) Determine how the reactive load power affects the control strategy;

(3) Incorporate a detailed fuel processor model and develop a controller for the fuel

processor and the fuel cell stack.

CHAPTER 5 REFERENCES

[1] Hajizadeh, M.A. Golkar, Intelligent power management strategy of hybrid distributed generation system, International Journal of Electrical Power and Energy Systems 29 (10) (2007) 783–795

[2] Caisheng Wang, Load transient mitigation for stand-alone fuel cell power generation systems, IEEE Transactions on Energy Conversion 22 (4) (2007) 864–872

[3] C.A. Ramos, Maximum power point tracking strategy for fuel cell power systems, in: 2007 Industrial Electronics Conference, June 2007, pp.2613–2618

[4] Song-Yul Choe, Jung-Gi Lee, Integrated modeling and control of a PEM fuel cell power system with a PWM DC/DC converter, Journal of Power Sources 164 (2) (2007) 614–623

[5] Jeong Kwi-Seong, Lee Won-Yong, Kim Chang-Soo, Energy management strategies of a fuel cell/battery hybrid system using fuzzy logics, Journal of Power Sources 145 (2) (2005) 319–326

[6] Marco Amrhein, Dynamic Simulation for Analysis of Hybrid Electric Vehicle System and Subsystem Interactions Including Power Electronics, IEEE Transactions on Vehicular Technology 54 (3) (2005) 825–836

[7] J. Padullés, G. W. Ault, J. R. McDonald An integrated SOFC plant dynamic model for power systems simulation, Journal of Power Sources 86 (1) (2000) 495–500

[8] Zhi-dan Zhong, Hai-bo Huo, Xin-jian Zhu, Guang-yi Cao, Adaptive maximum power point tracking control of fuel cell power plants, Journal of Power Sources 176 (1) (2008) 259–269

[9]   X.D. Xue, K.W.E. Cheng, D. Sutanto, Unified mathematical modeling of steady-state and dynamic voltage–current characteristics for PEM fuel cells, Electrochimica Acta 52 (3) (2006) 1135–1144

[10]   M. Uzunoglu, Dynamic modeling, design, and simulation of a combined PEM fuel cell and ultra capacitor system for stand-alone residential applications, IEEE Transactions on Energy Conversion 21 (3) (2006) 767–775

[11]   Brad Bryant, Open-loop power-stage transfer functions relevant to current-mode control of boost PWM converter operating in CCM, IEEE Transactions on Circuits and Systems 52 (10) (2005) 2158–353

[12]   Hanifi Guldemir, Sliding mode control of DC-DC boost converter, Journal of Applied Sciences 5 (3) (2005) 588–592

[13]   Fei Zhang, Guangjun Liu, A Battery State of Charge Estimation Method with Extended Kalman Filter, in: International Conference on Advanced Intelligent Mechatronics, July 2008, pp.1008–1013

[14]   A. Vasebi , Predicting state of charge of lead-acid batteries for hybrid electric vehicles by extended Kalman filter, Energy Conversion and Management 49 (1) (2008) 75–82

[15]   Peng Li, Zhang Yu, Kang Yong, Chen Jian, Design Method of Analog Controller for High-performance Inverter, Proceedings of the CSEE 26 (6) (2006) 89–94

[16]   Dawei Gao, Energy management strategy based on fuzzy logic for a fuel cell hybrid bus, Journal of Power Sources 185 (1) (2008) 311–317

[17]   Chun-Yan Li, Guo-Ping Liu, Optimal fuzzy power control and management of fuel cell/battery hybrid vehicles, Journal of Power Sources 192 (2) (2009) 525–533

CHAPTER 6 APPENDIX

DCDC.m
%design PI controller for Gid

m=8;n=8;G=0.7;Wr=3000;

%circuit parameters
R = 2; L = 100*1e-6; C = 400*1e-6;V=100;D=0.7;

%PI controller for the booster equation (2-15)
Wp=((m+n+2)*G*Wr*R*L*C-L)/(R*L*C);
Wi=((m*n*G*G*Wr*Wr+2*(m+n)*G*G*Wr*Wr+Wr*Wr)*(R*L*C)-R*(1-D)*(1-D)-L*Wp)/(V*R*C);
Wz=((2*m*n*(G*Wr)*(G*Wr)*(G*Wr)+Wr*Wr*Wr*(m+n)*G)*(R*L*C)-Wp*R*(1-D)*(1-D)-
2*V*Wi)/(V*R*C*Wi);
G2 = tf([Wi Wz*Wi],[1 Wp 0]);

%open loop transfer function
G = tf([V*R*C 2*V],[R*L*C L R*(1-D)*(1-D)]);%Gid
bode(G2*G), grid

Wp=3.655e+04
Wi=3.844e+02
Wz=1.156e+03

Gvi= tf([-R*L*   V*R*(1-D)],[V*R*C 2*V]);

DCAC.m
%design dual-loop controller for signal phase inverter

%circuit parameters
L=0.43*1E-3;
C=140*1E-6;
r=0.1;

%PID parameters
K1P=0.6;
K1I=970;
K2P=19;
K2I=156000;

%transfer function
Gvv= tf([K1P*K2P K1P*K2I+K1I*K2P K1I*K2I],[L*C   (C*r+C*K2P) (1+K1P*K2P+C*K2I)
(K1P*K2I+K2P*K1I) (K1I*K2I)]);

%Bode plot
bode(Gvv)
grid on
margin(Gvv)

SOC.m
```
% s function for SOC estimator
function [sys,x0,str,ts] = soc(t,x,u,flag)
%
switch flag,

  %%%%%%%%%%%%%%%%%%
  % Initialization %
  %%%%%%%%%%%%%%%%%%
  case 0,
    [sys,x0,str,ts]=mdlInitializeSizes;

  %%%%%%%%%%%%%%%
  % Derivatives %
  %%%%%%%%%%%%%%%
  case 1,
    sys=mdlDerivatives(t,x,u);

  %%%%%%%%%%
  % Update %
  %%%%%%%%%%
  case 2,
    sys=mdlUpdate(t,x,u);

  %%%%%%%%%%%
  % Outputs %
  %%%%%%%%%%%
  case 3,
    sys=mdlOutputs(t,x,u);

  %%%%%%%%%%%%%%%%%%%%%%%%
  % GetTimeOfNextVarHit %
  %%%%%%%%%%%%%%%%%%%%%%%%
  case 4,
    sys=mdlGetTimeOfNextVarHit(t,x,u);

  %%%%%%%%%%%%%
  % Terminate %
  %%%%%%%%%%%%%
  case 9,
    sys=mdlTerminate(t,x,u);

  %%%%%%%%%%%%%%%%%%%
  % Unexpected flags %
  %%%%%%%%%%%%%%%%%%%
  otherwise
    DAStudio.error('Simulink:blocks:unhandledFlag', num2str(flag));

end

% end sfuntmpl

%
%=========================================================================
==
% mdlInitializeSizes
```

```matlab
% Return the sizes, initial conditions, and sample times for the S-function.
%================================================================
==
%
function [sys,x0,str,ts]=mdlInitializeSizes

%
% call simsizes for a sizes structure, fill it in and convert it to a
% sizes array.
%
% Note that in this example, the values are hard coded.  This is not a
% recommended practice as the characteristics of the block are typically
% defined by the S-function parameters.
%
sizes = simsizes;

sizes.NumContStates  = 0;
sizes.NumDiscStates  = 2;
sizes.NumOutputs     = 2;
sizes.NumInputs      = 2;
sizes.DirFeedthrough = 1;
sizes.NumSampleTimes = 1;   % at least one sample time is needed

sys = simsizes(sizes);

%
% initialize the initial conditions
%
x0  = [0.6;0];

%
% str is always an empty matrix
%
str = [];

%
% initialize the array of sample times
%
ts  = [0.1 0];

% end mdlInitializeSizes

%
%================================================================
==
% mdlDerivatives
% Return the derivatives for the continuous states.
%================================================================
==
%
function sys=mdlDerivatives(t,x,u)

sys = [];

% end mdlDerivatives
```

```
%
%===============================================================================
==
% mdlUpdate
% Handle discrete state updates, sample time hits, and major time step
% requirements.
%===============================================================================
==
%
function sys=mdlUpdate(t,x,u)

Ccb=11252.4;
Ccs=27.31;
Ri=0.1174;
Rt=0.1645;
k=5.38;
d=23.74;

Tc=1/10;


%K=[0.0032;0.1451];%measurement noise=2
 K=[0.0059;0.2786];%measurement noise=1
 fxhat=[u(1)/(k*Ccb);
       -x(2)/(Rt*Ccs)+u(1)/Ccs];
    x=x+fxhat;
     %State estimate measurement update
     x=x+K*(u(2)-(k*x(1)+x(2)+Ri*u(1)+d));
    % Error covariance measurement update
sys = x;

% end mdlUpdate

%
%===============================================================================
==
% mdlOutputs
% Return the block outputs.
%===============================================================================
==
%
function sys=mdlOutputs(t,x,u)

sys = x;

% end mdlOutputs

%
%===============================================================================
==
% mdlGetTimeOfNextVarHit
% Return the time of the next hit for this block.  Note that the result is
% absolute time.  Note that this function is only used when you specify a
% variable discrete-time sample time [-2 0] in the sample time array in
% mdlInitializeSizes.
```

```
%========================================================================
==
%
function sys=mdlGetTimeOfNextVarHit(t,x,u)

sampleTime = 1;    %  Example, set the next hit to be one second later.
sys = t + sampleTime;

% end mdlGetTimeOfNextVarHit

%
%========================================================================
==
% mdlTerminate
% Perform any end of simulation tasks.
%========================================================================
==
%
function sys=mdlTerminate(t,x,u)

sys = [];

% end mdlTerminate
```

Fuzzylogic.m
```
%creation of a fuzzy logic controller
clear all;
clc;
close all;
global a;
a=newfis('powermanagement');
a=addvar(a,'input','soc',[0,1]);              % Parameter soc
a=addmf(a,'input',1,'VL','trapmf',[0,0,0.4,0.55]);
a=addmf(a,'input',1,'L','trimf',[0.4,0.55,0.6]);
a=addmf(a,'input',1,'M','trimf',[0.55,0.6,0.65]);
a=addmf(a,'input',1,'H','trimf',[0.6,0.65,0.8]);
a=addmf(a,'input',1,'VH','trapmf',[0.65,0.8,1,1]);

a=addvar(a,'input','power demand',[0,1]);      % Parameter power demand
a=addmf(a,'input',2,'L','trapmf',[0,0,0.1,0.5]);
a=addmf(a,'input',2,'M','trimf',[0.1,0.5,0.9]);
a=addmf(a,'input',2,'H','trapmf',[0.5,0.9,1,1]);

a=addvar(a,'output','power required',[0,1]); % Parameter power required
a=addmf(a,'output',1,'L','trapmf',[0,0,0.1,0.35]);
a=addmf(a,'output',1,'M','trimf',[0.1,0.35,0.6]);
a=addmf(a,'output',1,'H','trimf',[0.35,0.6,0.85]);
a=addmf(a,'output',1,'VH','trapmf',[0.6,0.85,1,1]);


rulelist=[1 1 3 1 1;                      % Edit rule base
      1 2 3 1 1;
      1 3 4 1 1;
      2 1 2 1 1;
      2 2 3 1 1;
      2 3 4 1 1;
      3 1 1 1 1;
      3 2 2 1 1;
      3 3 3 1 1;
      4 1 1 1 1;
      4 2 1 1 1;
      4 3 2 1 1;
      5 1 1 1 1;
      5 2 1 1 1;
      5 3 1 1 1;
     ];

a=addrule(a,rulelist);
%showrule(a)              % Show fuzzy rule base
a1=setfis(a,'DefuzzMethod','centroid');  % Defuzzy
a=readfis('ljk');
%plotfis(a2);[-4.5,x_pop(3),1.5]
h2=a;
plotfis(h2)


subplot(3,1,1);
plotmf(h2,'input',1);
xlabel('SOC');
ylabel('');
```

```
set(gca,'FontSize',12); set(gcf,'Color','White');

subplot(3,1,2);
plotmf(h2,'input',2);
xlabel(Average load power');
ylabel('Degree of membership');
set(gca,'FontSize',12); set(gcf,'Color','White');

subplot(3,1,3);
plotmf(h2,'output',1);
xlabel('Fuel cell output power');
ylabel(");
set(gca,'FontSize',12); set(gcf,'Color','White');

figure;
gensurf(h2);
set(gca,'FontSize',12); set(gcf,'Color','White');
xlabel('SOC');
ylabel('Filtered load power');
zlabel('Fuel cell output power');
```